Detection of uncoupled circadian rhythms in individual cells of *Lemna minor* by using a dual-color bioluminescence monitoring system

Emiri Watanabe, Minako Isoda, Tomoaki Muranaka[1], Shogo Ito, and Tokitaka Oyama

Department of Botany, Graduate School of Science, Kyoto University, Kitashirakawa-oiwake-cho, Sakyo-ku, Kyoto 606-8502, Japan

[1]Present address: Faculty of Agriculture, Kagoshima University, Kohrimoto 1-21-24, Kagoshima 890-0065, Japan.

Correspondence should be addressed to T. O. (oyama@cosmos.bot.kyoto-u.ac.jp).

Abstract

The plant circadian oscillation system is based on the circadian clock of individual cells and coordinates the circadian behavior of the plant body. To observe cellular circadian behavior of both the oscillator and its output in plants, we developed the dual-color bioluminescence monitoring system that automatically measured the luminescence of two luciferase reporters simultaneously at a single-cell level. We selected a yellow-green-emitting firefly luciferase (LUC+) and a red-emitting luciferase (PtRLUC) that is a mutant form of Brazilian click beetle ELUC. We used *AtCCA1::LUC+* and *CaMV35S::PtRLUC* to observe cellular behavior of oscillator and output, respectively. These bioluminescent reporters were introduced into cells of a duckweed, *Lemna minor*, by particle bombardment. Time series of bioluminescence of individual cells in a frond were obtained by the dual-color bioluminescence monitoring system with a green-pass- and a red-pass filter. Luminescence intensities from LUC+ and PtRLUC of each cell were calculated from the filtered luminescence intensities. We succeeded in reconstructing bioluminescence behaviors of *AtCCA1::LUC+* and *CaMV35S::PtRLUC* in the same cells. Under prolonged constant light conditions, *AtCCA1::LUC+* showed a robust circadian rhythm in individual cells in an asynchronous state in the frond, as previously reported in studies using other plants. In contrast, *CaMV35S::PtRLUC* stochastically showed circadian rhythms in a synchronous state. Thus, we clearly demonstrated the uncoupling between oscillator and output in individual cells. This dual-color bioluminescence monitoring system is a powerful tool to analyze various stochastic phenomena accompanying large cell-to-cell variation in gene expression.

Keywords

Bioluminescence; Circadian clock; Luciferases; Duckweed; Single-cell monitoring; Particle bombardment; *CCA1*; *CaMV35S*; Uncoupled rhythms

Introduction

Many physiological phenomena in plants show daily rhythms under day/night cycles, and they show circadian rhythms even under constant conditions. The circadian clock is composed of a number of clock genes that form transcription-translation feedback loops in individual cells (Nagel and Kay, 2012). Thus, the circadian clock is basically a cell-autonomous system. These concepts have been led by various studies using bioluminescence monitoring techniques (Muranaka and Oyama, 2018). Bioluminescence rhythms of transgenic plants expressing a firefly luciferase under the control of circadian promoters are monitored using a photomultiplier tube or a high-sensitive camera. Bioluminescence imaging of transgenic plants can spatially distinguish circadian rhythms in a plant body or a specific organ; damping (spontaneous desynchronization) of bioluminescence rhythms of a region and asynchronous rhythms in an organ has been clearly shown (Fukuda *et al.*, 2007; Fukuda *et al.*, 2012; Wenden *et al.*, 2012). These observations suggested heterogeneous circadian behavior among cells even in the same tissue. The heterogeneity was quantitatively demonstrated by the observation of bioluminescence circadian rhythms at a single-cell level in duckweed plants (Muranaka *et al.*, 2013; Muranaka and Oyama, 2016; Okada *et al.*, 2017; Isoda and Oyama, 2018). A bioluminescent reporter, *AtCCA1::LUC+* was used for gene transfection to cells by a particle bombardment method. The *Arabidopsis CCA1* gene is one of the clock genes and highly expressed around dawn (Wang and Tobin, 1998). CCA1 is widely conserved among plants and its function in the circadian rhythm is also conserved (Miwa *et al.*, 2006; Serikawa *et al.*, 2008; McClung, 2013; Linde *et al.*, 2017). This reporter activity which shows a robust circadian rhythm with a high amplitude (Nakamichi *et al.*, 2004; Muranaka *et al.*, 2015) was monitored for circadian rhythms of individual cells by using the automated imaging system with an EM-CCD camera (Muranaka *et al.*, 2013; Muranaka and Oyama, 2020). Duckweeds are suitable for imaging of an entire plant because of the tiny, flat, floating bodies. In addition, duckweed fronds (leaf-like structure) become immobile in the vertical direction, making it unnecessary to adjust the focus during long-term monitoring (Hillman, 1961; Muranaka *et al.*, 2013). Among duckweed species, *Lemna gibba* has been used for studies of circadian rhythms for a long time (Muranaka and Oyama, 2018). Recently, *Lemna minor*, which is phylogenetically close to *L. gibba*, has been used for various studies of duckweeds because the efficient genetic transformation system has been established and the genome sequence information is available (Chhabra *et al.*, 2011; Van Hoeck *et al.*, 2015).

As a basis of clock regulation of plant physiology, a relatively large number of genes are regulated by the circadian clock (Covington *et al.*, 2008; Michael *et al.*, 2008). Among these clock-regulated genes, large variation in peak phases, amplitudes, and waveforms are observed. They are likely to be regulated by other signals such as light, temperature, developmental events; gene expression of many of them are altered in tissues, developmental stages, and environmental conditions. Variation in circadian behavior of gene expression among genes has been studied in detail by monitoring transgenic plants carrying a circadian bioluminescent reporter (Thain *et al.*, 2000; Hall *et al.*, 2002; Michael and McClung, 2002; Thain *et al.*, 2002; Muranaka and Oyama, 2018). Although the variation or heterogeneity in the circadian behavior occurs in individual cells, comparative analysis among circadian-regulated genes has not performed at the single-cell level. Analysis of correlation of circadian traits (phase, period, stability, etc.) between various circadian behaviors at a single-cell level should be necessary to

reveal the cell-autonomous basis of the circadian system. Especially, cells that are asynchronous in a tissue in a plant are an interesting target of the analysis. A dual-color bioluminescence monitoring system is a tool to simultaneously detect expression levels of two reporter genes; circadian activities of different promoters of cyanobacteria and a mouse have been analyzed using this system (Kitayama *et al.*, 2004; Nakajima *et al.*, 2004; Nakajima *et al.*, 2005; Ogura *et al.*, 2005; Kwon *et al.*, 2010; Nishide *et al.*, 2018). Simultaneous detection of cellular circadian rhythms of two bioluminescent reporters was only reported for mammalian cultured cells (Kwon *et al.*, 2010). Kwon et al. developed a dual-path optical luminescence imaging system and simultaneously tracked two circadian gene expression patterns for several days in a single-cell. They used two luciferases: a green-emitting ELuc derived from *Pyrearinus termitilluminans*, and a red-emitting SLR derived from *Phrixothrix hirtus*. Bioluminescence of single cells that were transfected with two mammalian clock-gene reporters showing different phases was separated to green- and red-color images by using dichroic mirrors and was imaged on the CCD sensor in the microscope system.

In this study, we developed a dual-color bioluminescence monitoring system that enabled us to approach different circadian traits in individual cells in a plant. Based on the single-cell bioluminescence imaging system that was previously developed (Muranaka and Oyama, 2016), we set the filter changer that was used to separate luminescence from different color luciferases in the same sample. As the luciferase reporters, we chose the commonly-used firefly luciferase (LUC+) and PtRLUC that is a red-shift mutant (S246H/H347A) of ELuc from *Pyrearinus termitilluminans* (Nishiguchi *et al.*, 2015). LUC+ and PtRLUC emit yellow-green (λmax = ~560 nm) and red (λmax = 602 nm) luminescence, respectively. As a robust circadian bioluminescent reporter, we chose *AtCCA1::LUC+* that was used for the observation of circadian rhythms at a single-cell level in a duckweed plant (Muranaka *et al.*, 2013; Muranaka and Oyama, 2016; Okada *et al.*, 2017; Isoda and Oyama, 2018). This reporter activity basically represents the behavior of the circadian clock in individual cells; it is regarded as a direct output of the cellular oscillator. As an output reporter with a circadian rhythm, we chose PtRLUC driven by the *CaMV35S* promoter. While the *CaMV35S* promoter is known as a constitutive promoter, the *CaMV35S::LUC+* reporter showed a bioluminescence circadian rhythm in duckweed plants under constant light after light/dark cycles (Muranaka *et al.*, 2015). *CaMV35S* is a virus-derived promoter that is not directly related to the clock oscillation and can be thought of as an output downstream of the clock. By co-transfecting cells in *L. minor* with *AtCCA1::LUC+* and *CaMV35S::PtRLUC*, we succeeded in monitoring two reporter activities in individual cells of a plant. Results of the dual-color bioluminescence monitoring system clearly indicated the uncoupling of circadian rhythms between *AtCCA1::LUC+* and *CaMV35S::PtRLUC* in the same cells.

Results

Characterization of bioluminescence of cells expressing LUC+ or PtRLUC in *Lemna minor*

We first confirmed that the transfection procedure of particle bombardment for *L. gibba* worked on *L. minor* (Figure S1 a). The major target of this transfection was epidermal cells (Figure S1 b, c). Approximately 70% of transfected cells in fronds were epidermal cells and the remainder were mesophyll cells. Then, by using an automatic luminescence monitoring system with photomultiplier tubes, we roughly confirmed that *LUC+* and

PtRLUC under the *CaMV35S* promoter introduced into *L. minor* showed a circadian rhythm similarly to *CaMV35S::LUC+* reported in *L. gibba* (Figure S2, Muranaka *et al.*, 2015). As reported for *CaMV35S::LUC+* in *L. gibba*, *CaMV35S::LUC+* and also *CaMV35S::PtRLUC* in *L. minor* showed circadian rhythms under constant light after light/dark cycles at a whole plant level (Figure S2 a, b). On the other hand, both reporters in *L. minor* plants without having experienced any light/dark cycles showed almost no circadian rhythmicity (Figure S2 c, d). Thus, *CaMV35S::LUC+* and *CaMV35S::PtRLUC* showed similar bioluminescence traces in *L. minor*.

In order to separately monitor bioluminescence of LUC+ and PtRLUC in the same cells, we set up a dual-color bioluminescence imaging system. As shown in Figure 1a, we set a filter changer to the single-cell bioluminescence imaging system that was reported previously (Muranaka and Oyama, 2016). Using this system, we roughly examined the luminescence spectra of these two luciferases (Figure 1b). A plasmid construct expressing a luciferase gene under the *CaMV35S* promoter was used for gene transfection to cells in *L. minor* plants by particle bombardment. One day after the transfection, bioluminescence intensities of a frond were measured with a series of optical band-pass filters. In plant cells, maximum emission wavelengths were around 560 nm and 600 nm for LUC+ and PtRLUC, respectively. Based on the spectra of luminescence, we selected a set of band-pass filters for LUC+ (green-pass filter: 490–570 nm) and for PtRLUC (red-pass filter: 610–650 nm). Foci of an image were altered when those filters were set (Figure 1a). The focus for each filter was optimized by adjusting the distance between the sample and the lens by driving a z-axis motor for the stage. Figure 1c shows an example of a set of images for an *AtCCA1::LUC+*-transfected frond and a *CaMV35S::PtRLUC*-transfected frond at a time in monitoring. Exposure times for each image were optimized to obtain luminescence within an appropriate range. These sets of images were captured every 1 h and individual luminescence spots were quantified for each filtered image. Figure 1d shows a set of time series data of luminescence intensity of a spot (green arrow in Figure 1c) in the *AtCCA1::LUC+*-transfected plant under constant light conditions (Exp1-1 in Table S1). Intensities of luminescence captured without a filter (hereafter unfiltered luminescence intensities, L; gray line) showed a robust circadian rhythm for a week. Intensities of luminescence transmitted through the green-pass filter (hereafter green luminescence intensities, L_g; green line) also showed a robust circadian rhythm with a similar waveform to that of unfiltered luminescence intensities. Intensities of luminescence transmitted through the red-pass filter (hereafter red luminescence intensities, L_r; red line) were much lower than unfiltered luminescence intensities but showed a circadian rhythm. Figure 1e shows a set of time-series data of luminescence intensity of a spot (red arrow in Figure 1c) in the *CaMV35S::PtRLUC*-transfected plant under constant light conditions (Exp2-1 in Table S1). Unfiltered luminescence intensities (gray line) showed a low-amplitude circadian rhythm with high-frequency noise. Compared to the unfiltered luminescence intensities, green luminescence intensities (green line) were close to zero. Red luminescence intensities (red line) showed a circadian rhythm with a similar waveform to that of unfiltered luminescence intensities.

Calculation to separately monitor bioluminescence of LUC+ and PtRLUC in the same cells

First, we quantitively analyzed the transmittance of the filters by using time-series data of the *AtCCA1::LUC+* transfected cells (Exp1-1 in Table S1). The transmittance of a data point for the two filters (L_g/L for the green-pass filter, L_r/L for the red-pass filter) was calculated for those data with $L > 1000$ photons/s. The time series of

AtCCA1::LUC+ luminescence included data with very low intensities due to its high amplitude rhythm, and the transmittance of those datapoints were widely distributed due to near the background level of their unfiltered- and/or filtered luminescence intensities (Figure S3a). Figure 2a shows histograms for the transmittance for the green-pass filter (green bins) and the red-pass filter (red bins). The transmittance of LUC+ was normally distributed for both filters, with an average of 0.49±0.06 for the green-pass filter (Kolmogorov-Smirnov, P = 0.62) and 0.09±0.02 for the red-pass filter (Kolmogorov-Smirnov, P = 0.25). The normal distribution suggests that these mean values can be used as the representative values of their transmittance. The scatter plot of green- and red-pass filter transmittance for each data point shows uncorrelation between them (Figure 2b). Note that the transmittance of LUC+ appears to be affected by the expression level (Figure S4). Luminescence intensities of *CaMV35S::LUC+* expressing cells were ~100 times larger than those of *AtCCA1::LUC+*, and the transmittance of *CaMV35S::LUC+* looked to be smaller and larger for green-pass- and red-pass filter, respectively. Then, we quantitively analyzed the transmittance of the filters by using time-series data of the *CaMV35S::PtRLUC* transfected cells (Exp2-1 in Table S1). Luminous spots showed strong emission and did not include those with intensities near the background (Figure S3b). The transmittance of PtRLUC was normally distributed for the red-pass filter with an average of 0.26±0.03 (Kolmogorov-Smirnov, P = 0.51) (Figure 2c). The transmittance for the green-pass filter was low with an average of 0.045±0.007. The Kolmogorov-Smirnov p-value for the transmittance of the green-pass filter is very low (P = 0.00), suggesting that the distribution is not a normal distribution (Figure 2c). This seems to be due to the difficulty in obtaining exact values of the transmittance for individual spots with very low intensities of green-filtered luminescence. The scatter plot of green- and red-pass filter transmittance for each data point shows uncorrelation between them (Figure 2d). For these reasons, we used these mean values as the representative values of their transmittance.

Next, we gave a calculation formula to estimate luminescence intensities from two luciferases (L_{LUC+}, L_{PtRLUC}) in the same cells from the filtered luminescence intensities (L_g, L_r). As explained in Figure S5,

$$\begin{pmatrix} L_{LUC+} \\ L_{PtRLUC} \end{pmatrix} = A^{-1} \begin{pmatrix} L_g \\ L_r \end{pmatrix}$$

in which the elements of matrix A are transmittance for the combinations of luciferases and filters. To confirm the formula worked well, time-series data of estimated luminescence intensities were compared with those of unfiltered luminescence intensities (L) for the cells separately transfected with *AtCCA1::LUC+* (Exp1-1 in Table S1) or *CaMV35S::PtRLUC* (Exp2-1 in Table S1). As shown in Figure 2e and S6 on the whole, L_{LUC+} values in time-series of *AtCCA1::LUC+* transfected cells matched with L, and L_{PtRLUC} values were close to 0. Thus, the formula worked well to reconstruct *AtCCA1::LUC+* luminescence from the filtered luminescence intensities. However, at time points with strong intensities (L > ~5000 photons/s), the L_{LUC+}- and L_{PtRLUC} values tended to be underestimated and overestimated, respectively (arrows in Figure S6). This looked to be caused by the expression-level-dependent alteration of transmittance of LUC+ (Figure S4). Thus, it would be better to use an appropriate matrix for the calculation dependent on the expression level of LUC+. As shown in Figure 2f and S7, L_{PtRLUC} values in time series of *CaMV35S::PtRLUC* transfected cells well matched with L, and L_{LUC+} values were kept close to 0. Thus, the formula worked well to reconstruct *CaMV35S::PtRLUC* luminescence from the filtered luminescence intensities. Therefore, we concluded that the calculation formula was practically used for the

estimation of luminescence intensities from two luciferases in co-transfected cells of *AtCCA1::LUC+* and *CaMV35S::PtRLUC*.

Estimation of luminescence intensities of the two reporters in the co-transfected cells

We measured the luminescence of the cells co-transfected with the two reporters, with and without filters in a time series. Figure 3a shows an example of a luminous spot exhibiting a circadian rhythm. Red luminescence intensities were larger than green luminescence intensities in most time points. Figure 3b shows a plot of transmittance of the green- and red-pass filters at every time point for the spot. In the plot, the green- and red crosses show the representative values of the transmittance for LUC+ and PtRLUC luminescence, respectively (see Figure 2b, d). Points on the line segment connecting these crosses (blue line) satisfy the condition where the sum of L_{LUC+} and L_{PtRLUC} is L when L_{LUC+} and L_{PtRLUC} are reconstructed using the calculation formula. Data points distribute close to the line segment, suggesting that the calculation formula works to estimate luminescence intensities of the two reporters in the same cell. Note that many data points are around the endpoint of the line segment (red cross) because the PtRLUC luminescence dominated over LUC+ luminescence for this cell. Figure 3c shows the time series of reconstructed luminescence intensities of the two reporters for this cell. Both *AtCCA1::LUC+* and *CaMV35S::PtRLUC* showed circadian rhythms while luminescence intensities of *CaMV35S::PtRLUC* were larger than those of *AtCCA1::LUC+* in most time points. As observed in single reporter transfection experiments, *CaMV35S::PtRLUC* showed a low-amplitude rhythm with high frequency noise and *AtCCA1::LUC+* showed a high amplitude rhythm. The *AtCCA1::LUC+* rhythm appears to include a jaggy noise probably due to the partial interference of *CaMV35S::PtRLUC* luminescence.

Figure S8 shows the time series of reconstructed luminescence intensities of the two reporters for 34 cells in a frond (Exp3-1). For each cell, overall luminescence of time series of *CaMV35S::PtRLUC* was larger than that of *AtCCA1::LUC+*; the difference varied among cells. Based on the results obtained from single reporter transfection experiments, we decided the following three criteria for luminous spots that were used for time-series data analysis of both reconstructed luminescence (Figure S9). (1) Spots with extremely low expression levels of either reporter were removed. (2) Spots showing too strong expression of LUC+ were removed because of the expression-level-dependent alteration of its transmittance for filters. (3) Spots with luminescence ratios of LUC+ and PtRLUC in an appropriate range were selected. The number of analyzable luminous spots varied among co-transfection experiments; 3 to 20 cells were selected in 6 independent experiments (Figure S8, Table S1).

Evaluation of reconstructed bioluminescence traces of the two reporters in co-transfection experiments

We first performed rhythm analysis on bioluminescence traces by following the scheme in Figure S9. The free-running period (FRP) and relative amplitude error (RAE) of each luminescence trace were calculated using the FFT-NLLS method (Plautz *et al.*, 1997). The RAE value represents the degree of confidence of rhythmicity, ranging from 0 (complete sine-fitting) to 1 (arrhythmic). In this analysis, bioluminescence traces with RAE < 0.2 is defined as rhythmic, and the rest are defined as arrhythmic (Figure S10). In single reporter transfection experiments for *AtCCA1::LUC+*, bioluminescence traces of most cells showed high amplitude rhythms (Figure S6), and the proportion of rhythmic traces to analyzable ones ranged from 0.93 to 0.97 in four independent experiments (Figure

4a). Thus, every cell in *L. minor* basically show a self-sustained circadian rhythm of this reporter under continuous light, as has been reported in *L. gibba* (Muranaka and Oyama, 2016). In contrast, luminous spots of *CaMV35S::PtRLUC* in single reporter transfection experiments showed traces with low amplitude circadian rhythms or without circadian rhythmicity (Figure S7), and the proportion of rhythmic traces to analyzable ones ranged from 0.29 to 0.55 in four independent experiments (Figure 4a). Note that bioluminescence traces of *CaMV35S::PtRLUC* judged as rhythmic (RAE < 0.2) showed lower amplitudes and rougher waveform than those of *AtCCA1::LUC+* (Figure S10). Thus, the circadian rhythm of *CaMV35S::PtRLUC* was unstable and the rhythmicity occurred stochastically in cells of non-entrained plants. Since the proportion of rhythmic cells for *CaMV35S::PtRLUC* was clearly lower than that for *AtCCA1::LUC+*, it was expected that *CaMV35S::PtRLUC* luminescence traces without circadian rhythmicity would be observed as well as those with it in cells with *AtCCA1::LUC+* rhythms in the co-transfection experiments.

In six co-transfection experiments of *AtCCA1::LUC+* and *CaMV35S::PtRLUC*, three experiments had more than 10 analyzable luminous spots for both reconstructed luminescence (Table S1). In these three experiments, the proportion of rhythmic traces of *AtCCA1::LUC+* to analyzable ones ranged from 0.74 to 0.90, while that of *CaMV35S::PtRLUC* ranged from 0.11 to 0.55 (Figure 4a). The proportion for *AtCCA1::LUC+* looked lower in co-transfection experiments than in single transfection ones. There appeared to be interference from *CaMV35S::PtRLUC* luminescence large enough to increase RAE values of *AtCCA1::LUC+* traces. In fact, reconstructed *AtCCA1::LUC+* luminescence traces in co-transfection experiments included large jaggy noises, which were often observed in *CaMV35S::PtRLUC* luminescence traces (Figure S6, S7, S8). As expected in single transfection experiments, in cells with *AtCCA1::LUC+* rhythms, *CaMV35S::PtRLUC* luminescence traces without circadian rhythmicity were observed as well as those with it. As shown in Figure 4b, d, f and Figure S8, some cells showed robust *AtCCA1::LUC+* rhythms and low amplitude *CaMV35S::PtRLUC* rhythms while some showed circadian rhythmicity only in *AtCCA1::LUC+*. Reconstructed *CaMV35S::PtRLUC* luminescence traces in co-transfection experiments appeared to be similar to those observed in single transfection experiments. In fact, peak times of reconstructed *CaMV35S::PtRLUC* luminescence traces occurred independently of those of *AtCCA1::LUC+* rhythms (Figure 4c, e, g). Thus, interference from *AtCCA1::LUC+* luminescence looked to be low enough to maintain the original properties of *CaMV35S::PtRLUC.* Taken together, it is demonstrated that luminescence behaviors of the two reporters can be simultaneously monitored in individual cells by using the dual-color bioluminescence monitoring system.

Uncoupling of circadian behavior between *AtCCA1::LUC+* and *CaMV35S::PtRLUC* in the same cells

While *AtCCA1::LUC+* reflects the behavior of cellular oscillator, the rhythm of *CaMV35S::PtRLUC* can be regarded as output of circadian oscillator (Muranaka *et al.*, 2015; Muranaka and Oyama, 2016). The presence of both cells with and without the *CaMV35S::PtRLUC* rhythm in the same frond indicates that the cellular output observed in *CaMV35S::PtRLUC* luminescence can be uncoupled from the cellular oscillator to behave arrhythmically. Generally, uncoupling of an output rhythm from the oscillator can be detected in inconsistency of the phase relationship between them. When the output rhythm is completely coupled with the cell oscillator, it is expected that every cell shows a similar phase relationship.

Figure 5a shows a plot of the peak time difference between *AtCCA1::LUC+* and *CaMV35S::PtRLUC* against the peak of the *AtCCA1::LUC+* rhythm for six cells with both rhythms in the same frond (Exp3-1 in Table S1). A positive value of the peak time difference represents that the phase of *AtCCA1::LUC+* is advanced to that of *CaMV35S::PtRLUC*, e.g. Figure 4b, c. A negative value represents that the phase of *AtCCA1::LUC+* is delayed to that of *CaMV35S::PtRLUC*, e.g. Figure 4d, e. When the phase relationship is consistent, the peak time difference is plotted horizontally. Instead, the phase relationship between *AtCCA1::LUC+* and *CaMV35S::PtRLUC* varied greatly among cells, as the time difference was distributed in the range from -12 to 6 h. The inconsistency of the phase relationship was also observed among 11 cells with both rhythms in another frond (Figure S11). Thus, the uncoupling of *CaMV35S::PtRLUC* from *AtCCA1::LUC+* was clearly shown in cells with both rhythms. This suggests that the *CaMV35S::PtRLUC* rhythm in a cell may not be generated by the cellular circadian oscillator. Although the peak time difference is distributed in the range from -12 to 6 h, the points look to be orderly scattered on lines with the slope of -1 on the plot (Figure 5a). This suggests that while the phase of *AtCCA1::LUC+* varies from cell to cell, the *CaMV35S::PtRLUC* rhythm is in phase among the six cells. Figure 5b shows the peak time distribution of *AtCCA1::LUC+* rhythm every day and its average phase and the degree of synchronicity. The average peak times looks similar each day, but the degree of synchronicity is very low. On the other hand, *CaMV35S::PtRLUC* rhythms in the six cells showed similar peak times on average and higher degrees of synchronicity compared with *AtCCA1::LUC+* (Figure 5c). The higher degree of synchronicity among *CaMV35S::PtRLUC* rhythms than that among *AtCCA1::LUC+* rhythms is also observed in another frond (Figure S11). Thus, it is shown that the *CaMV35S::PtRLUC* rhythm in individual cells is highly synchronous in a frond with asynchronous cellular oscillators.

In addition to the difference in synchronicity, the difference of the distribution of free running periods was observed between *AtCCA1::LUC+* and *CaMV35S::PtRLUC* rhythm of cells with both rhythms (Figure S12). Out of the 21 cells in the six co-transfection experiments, 17 cells showed a shorter period length in *CaMV35S::PtRLUC* rhythm than in *AtCCA1::LUC+* rhythm. Furthermore, the correlation coefficient between the two periods is r = -0.11, suggesting that the period of *CaMV35S::PtRLUC* rhythm may not be affected by that of the cellular oscillator in individual cells.

In sum, by using the dual-color bioluminescence monitoring system, we observed inconsistency of phase relationship, synchronicity, and periodicity between *AtCCA1::LUC+* rhythm and *CaMV35S::PtRLUC* rhythm in the same cells in a frond. Thus, we clearly demonstrate the uncoupling of an output rhythm from the cellular oscillator at the cell level.

Discussion

The plant circadian clock is a cell-autonomous oscillation system based on the transcription-translation feedback loop, and its time information is output via transcription control (Nagel and Kay, 2012). In a day/night cycle, each cellular oscillator is synchronized to its environment. Meanwhile, in the constant environment without any cue of day-night signals, those cellular oscillators tend to become desynchronized at the tissue/organ level in the same plant even though the circadian oscillation is maintained in individual cells (Fukuda *et al.*, 2007; Fukuda *et al.*,

2012; Wenden *et al.*, 2012; Muranaka and Oyama, 2016). Heterogeneity of cellular oscillators in the same tissue is an important force for the desynchronization (Muranaka and Oyama, 2016; Okada *et al.*, 2017; Muranaka and Oyama, 2018). It would be impossible to analyze the circadian system of individual cells in an asynchronous state by observing whole tissues/organs because the output should be arrhythmic at the tissue/organ level. Measuring simultaneously cellular behaviors both of the oscillator and output in the same cell should be a powerful tool to solve this problem. We developed a dual-color bioluminescence monitoring system that can monitor the luminescence of two reporters simultaneously at a single-cell level, and we clearly demonstrated the uncoupling between the cellular oscillator and output in the duckweed plant in an asynchronous state. Here, we introduced *AtCCA1::LUC+*, which reports the behavior of cellular oscillator with yellow-green luminescence, and *CaMV35S::PtRLUC*, which shows a circadian output with red luminescence (Muranaka *et al.*, 2015; Nishiguchi *et al.*, 2015; Muranaka and Oyama, 2016). By quantitative analysis on luminescence behaviors of these reporters in co-transfected cells, we obtained the following two pieces of evidence of the uncoupling between *AtCCA1::LUC+* and *CaMV35S::PtRLUC* rhythm. (1) Irrespective of the stability (presence or absence) of the *CaMV35S::PtRLUC* rhythm, *AtCCA1::LUC+* showed a robust rhythm basically in each cell. (2) Even in the frond with a low synchrony of cellular *AtCCA1::LUC+* rhythms, cellular *CaMV35S::PtRLUC* rhythms showed a relatively high synchrony. The uncoupling between these two rhythms could be supposed on the bases of the different proportions of rhythmic cells in the single transfection experiments (Figure 4a). However, it would be difficult to quantitatively analyze the relationship between these two rhythms by using data from the single transfection experiments because of the uncontrollable synchronicity of cellular circadian oscillators in plants without experiencing day/night cycles (Wenden *et al.*, 2012; Muranaka and Oyama, 2016).

In this study, we focused on cellular behaviors of *AtCCA1::LUC+* and *CaMV35S::PtRLUC* luminescence in a frond in an asynchronous state to exhibit advantages of the dual-color bioluminescence monitoring system. As shown in Figure S2, the circadian rhythmicity of *CaMV35S::PtRLUC* luminescence was depended on the synchronization in frond. The degree of synchrony of cellular circadian rhythms in plants/organs is an important factor for the entire circadian system (Masuda *et al.*, 2017; McClung, 2019). In general, a high degree of synchrony is required for the physiological function in timekeeping of plant. Interestingly, entrainment manners of cellular oscillators in *Arabidopsis* are presumed to be dependent on the degree of synchrony: the circadian rhythm of plants in an asynchronous state is more sensitive to a dark pulse for entrainment than that in a synchronous state (Masuda *et al.*, 2017). The circadian behavior of *CaMV35S::PtRLUC* luminescence seems to be a synchrony-dependent phenomenon and may be related to other synchrony-dependent phenomena. The mechanism to give the circadian rhythmicity to the luminescence of *CaMV35S::PtRLUC* is unknown. The uncoupling of the rhythm from the cellular oscillator suggests that *CaMV35S::PtRLUC* may not be directly controlled by the transcriptional and translational feedback loops of the oscillator, and the PtRLUC may be expressed without circadian rhythmicity. In fact, *CaMV35S* promoter is known as a constitutive promoter and its expression did not show a circadian rhythm in tobacco (Millar *et al.*, 1992). Similarly to *CaMV35S::PtRLUC*, *ZmUBQ::LUC+* showed a circadian luminescence rhythm in various duckweed plants (Muranaka *et al.*, 2015). *ZmUBQ* is known as a constitutive promoter for monocotyledonous plants (Christensen *et al.*, 1992; Miwa *et al.*, 2006). The circadian rhythms of these reporters observed in duckweed plants might be generated at the level of post-transcriptional regulation. It is known that

many gene products of plants are circadianly regulated at various post-transcriptional steps (McClung, 2019). Intracellular concentrations of substrates of luciferase are other possible factors that can be responsible for the circadian rhythms of these bioluminescent reporters. Firefly luciferase catalysis the ATP-dependent oxidation of luciferin (Van Leeuwen *et al.*, 2000). Circadian regulation of photosynthesis has been analyzed in many plant species (Dodd *et al.*, 2014). Production of ATP and oxygen is dependent on photosynthetic activity and changes in intracellular concentrations of these substrates of luciferase may be in a circadian manner. It was reported that ATP accumulation of *Lemna gibba* showed a circadian rhythm under constant light after light/dark cycles (Kondo and Nakashima, 1979). These molecules can diffuse through the apoplast or symplast, and their intracellular concentrations may be spatially equalized in a region of plant. Such diffusive molecules could be a mediator of cellular circadian rhythms that are uncoupled from the cellular oscillator but are locally synchronized with each other. In addition to these molecules derived from photosynthesis, it has been shown that there is a circadian rhythm in the absorption of ions, such as potassium and magnesium, and these diffusive ions may be involved in the circadian rhythmicity of luciferase reaction (Kondo and Tsudzuki, 1978; Kondo, 1983; Feeney *et al.*, 2016).

In this study, we used the firefly LUC+ as a short-wavelength luciferase in the dual-color bioluminescence monitoring system. Almost all of the bioluminescent transgenic plants carry this luciferase and its applications for plant science are widespread (Van Leeuwen *et al.*, 2000). They are preferably used in various analyses for gene expression dynamics. The enzymatic reaction of the firefly luciferase depends on the reaction conditions and its emission spectrum is altered by pH changes. Based on our single-cell transfection experiments using the firefly luciferase, it seems that the higher the expression level, the longer the emission wavelength (Figure S4). The enzyme reaction conditions may change due to the excess accumulation of luciferase. On the other hand, PtRLUC that we used as a long-wavelength luciferase appeared to show a similar emission spectrum independently of its expression level (Figure S3b). In our dual-color bioluminescence monitoring system, the selection of filters to separate luminescence between the two luciferases is critical. Ideally, the green-pass- and red-pass filters should transmit luminescence only from LUC+ and PtRLUC, respectively, and the band-pass range of each filter should include the wavelength of maximum emission intensity of each luciferase. Due to the overlap of the emission spectra between LUC+ and PtRLUC (Figure 1b), we had to use filters deviated from the ideal and had to select those cells only with good proportions of luminescence intensities between two reporters. A combination of luciferases with a smaller overlap of their emission spectra is preferable. Using a luciferase with maximum emission at a shorter wavelength than firefly LUC+ (λmax = ~560 nm) is an option; there are several available insect-derived luciferases (and their derivatives) in this category (λmax < ~550 nm) (Viviani, 2002). Treating plants with the same substrate, luciferin, for insect-derived luciferases is critical to ensure the homogeneous enzyme reaction conditions for the two luciferases in cells. In dual-color bioluminescence monitoring experiments previously reported for mammals and cyanobacteria, insect-derived luciferases in the shorter wavelength category were utilized (Kitayama *et al.*, 2004; Nakajima *et al.*, 2004; Nakajima *et al.*, 2005; Ogura *et al.*, 2005; Kwon *et al.*, 2010; Nishide *et al.*, 2018).

The dual-color bioluminescence monitoring system at a single-cell level is useful to deeply analyze the relationship (e.g., correlation) between two gene-expression behaviors. Especially stochastic phenomena found in gene expression (reporter activities) are interesting targets of the analysis using this monitoring system (Kærn *et al.*,

2005). In this study, circadian rhythmicity of *CaMV35S::PtRLUC* and phases of *AtCCA1::LUC+* rhythms are such stochastic phenomena. Various stochastic phenomena accompanying large cell-to-cell variation in plants have been difficult to approach their underlying regulatory networks. The dual-color bioluminescence monitoring system at a single-cell level should become an experimental tool to directly analyze the behavior of components in the networks. While we analyzed the luminescence behaviors of two reporters at the single-cell level in this study, similar analysis on stochastic phenomena found in larger spatial regions, such as within- and between individual variations can be performed by using transgenic plants expressing two luminescent reporters. It is known that under constant conditions transgenic *Arabidopsis* plants carrying the *AtCCA1::LUC* reporter exhibit a variety of spatiotemporal patterns of luminescent rhythms with significantly different phases even within the same organ (Fukuda *et al.*, 2007; Fukuda *et al.*, 2012; Wenden *et al.*, 2012). By combining another luminescent reporter for a clock- or output gene, the free-running circadian system at the tissue, organ, plant body levels should be deeply analyzed for its regulatory networks.

In this study, we used *L. minor* as the plant material. Since duckweeds are generally small and flat, they have been used for physiological experiments in the laboratory (Stomp, 2005; Muranaka and Oyama, 2018). In the studies on plant circadian rhythms, physiological rhythms, such as CO_2 output, ion uptake were well characterized by using duckweeds (Miyata and Yamamoto, 1969; Hillman, 1970; Kondo and Tsudzuki, 1978). Furthermore, functional analysis on clock-related genes in *Lemna* plants revealed the conservation of their gene functions in plants (Miwa *et al.*, 2006; Serikawa *et al.*, 2008; Okada *et al.*, 2017). Thus, knowledge about circadian systems including clock-related genes has been accumulated in duckweeds. Duckweed plants show a large diversity of structural complexity among species. The number of shoot apical meristems is one or two, and the existence of roots and tracheid tissue depends on species/genus (Les *et al.*, 1997). In *Arabidopsis*, the shoot apex and vascular tissues are regarded as a kind of pacemakers in the plant body (Fukuda *et al.*, 2007; Fukuda *et al.*, 2012; Endo *et al.*, 2014; Takahashi *et al.*, 2015). Their roles in the circadian system of plant will be approached by analyzing various duckweed plants. Basic circadian properties of various duckweed species have already analyzed by a bioluminescence monitoring system with particle bombardment (Muranaka *et al.*, 2015; Isoda and Oyama, 2018). The bioluminescence monitoring system at a single-cell level is also available in *Arabidopsis* leaves, and circadian rhythms of individual cells can be detected (Kanesaka *et al.*, 2019). In future, the dual-color bioluminescence monitoring system will be applied for the study of the circadian system in *Arabidopsis.*

Recently, methods of stable transformation of *L. minor* have been established (Chhabra *et al.*, 2011). Then, spatiotemporal analysis for circadian rhythm will be able to be performed using a transgenic duckweed carrying a circadian bioluminescent reporter similarly to that using *Arabidopsis*. Because duckweed grows flat on a liquid surface, it should be easier to monitor proliferating plants with a high resolution for a long time. By transiently introducing a circadian bioluminescent reporter by using particle bombardment into the transgenic duckweed, it will be possible to simultaneously observe the general behavior of the circadian rhythm in fronds and the circadian rhythm of individual cells. Analyzing combinations of various circadian reporters will lead to a deeper understanding of the complex circadian behavior in plants.

Methods

Plant material and growth conditions

Lemna minor 5512 was maintained in NF medium with 1% sucrose under constant light conditions in a temperature-controlled room (25±1°C) as previously described (Muranaka *et al.*, 2015). The white light (~20 µE $m^{-2}s^{-1}$) was supplied by fluorescent lamps (FLR40SEX-W/M/36-HG, NEC). Plants were grown on 60 ml of the medium in 200-ml Erlenmeyer flasks plugged with cotton. New stock cultures were made every week, and well-grown plants were used for experiments.

Luciferase reporter transfection by particle bombardment

As circadian bioluminescent reporters, we used *pUC-AtCCA1:: LUC+* (*AtCCA1::LUC+)* (Muranaka *et al.*, 2013), pUC18-CaMV35S::intron-luc+(*CaMV35S::LUC+*) (Muranaka *et al.*, 2015), and *pUC18-CaMV35S::PtRLUC* (*CaMV35S::PtRLUC*). *pUC18-CaMV35S::PtRLUC* is a reporter driven by *CaMV35S* promoter which expresses PtRLUC: a red shift mutant (S246H/H347A) of Emerald luciferase (ELuc) from Brazilian click beetle (*Pyrearinus termitilluminans*) (Nishiguchi et al., 2015). Reporter constructs were introduced into *L. minor* plants through particle bombardment as described previously (Muranaka *et al.*, 2015). In both single- and dual reporter experiments, the amounts of plasmid DNA for *AtCCA1::LUC+*, *CaMV35S::PtRLUC* and *CaMV35S::LUC+* were 2 µg, 0.2 µg and 0.2 µg, respectively.

Bioluminescence monitoring

The single-cell bioluminescence imaging was basically carried out as described previously (Muranaka and Oyama, 2016; Muranaka and Oyama, 2020), with modifications for dual-color bioluminescence- and multi-sample monitoring. Two colonies of *L. minor* transfected with a reporter(s) was transferred to a 35-mm polystyrene dish with 3 ml of growth medium containing 0.5mM D-luciferin. Two sample dishes (i.e, 4 colonies) were monitored at the same time. Sample dishes were set on a handmade motor-driven stage with rotation- and z-axis motors in the lightproof box in an incubator (25±1°C) (Muranaka and Oyama, 2020). The stage rotated to exchange positions of a sample underneath the lens of an EM-CCD camera (ImagEM C9100-13, Hamamatsu Photonics) or an end of optic fibers guiding LED light (approximately 30 µE $m^{-2}s^{-1}$). A handmade motor-driven filter changer with a rotation motor (ARS-4036-GM with a magnetic position sensor, Chuo Precision Industrial Co.) was set between the sample and the lens. A green-pass filter (PB0530/080 ϕ 49.7 mm, Asahi Spectra) and a red-pass filter (PB0630/040 ϕ 49.7 mm, Asahi Spectra) were set on slots in the filter changer, and a slot was left empty to capture unfiltered images. By controlling this imaging system with a PC software (HOKAWO, Hamamatsu Photonics), a series of bioluminescence images for a sample dish were automatically captured every 1 hour. Before image capture, we allowed at least 4 min of dark period for autofluorescence decay. After the dark period, images were captured for each filter condition: unfiltered, green-pass filtered, and red-pass filtered with the exposure time 20 s, 120 s, and 30 s, respectively. The focus for each filter condition was optimized by adjusting the distance between the sample and the lens by driving a z-axis motor of the stage. During the monitoring, the focal adjustment was performed as follows: from the reference position (unfiltered bioluminescence image in focus) 1.0-mm downward for the green-

pass filter and 1.8-mm downward for the red-pass filter. To remove cosmic ray spikes, two sequential images at a time for each filter condition were captured and the minimum value for each pixel was used for analysis. These exposure procedures accompanied an approximately 18-min dark period per hour.

Bioluminescence monitoring at a whole plant level (Figure S2) was performed as described previously (Muranaka *et al.*, 2015).

Time-series analysis

The bioluminescence intensity of each luminescent spot was measured as the integrated density of the region of interest (ROI; size, 6 × 6 pixels). Image analysis and postprocessing were carried out with ImageJ (http://rsbweb.nih.gov/ij/) as described previously (Muranaka and Oyama, 2020; Muranaka and Oyama, 2016). The following analysis was implemented by Python 3.7.4 (NumPy 1.16.5, SciPy 1.3.1). Terms and symbols for luminescence intensities are defined as follows.

Unfiltered luminescence intensity (L): Measured value of luminescence captured without a filter.

Green luminescence intensity (L_g): Measured value of luminescence transmitted through the green-pass filter.

Red luminescence intensity (L_r): Measured value of luminescence transmitted through the red-pass filter.

LUC+ luminescence intensity (L_{LUC+}): LUC+ luminescence value calculated from L_g and L_r.

PtRLUC luminescence intensity (L_{PtRLUC}): PtRLUC luminescence value calculated from L_g and L_r.

As explained in Figure S3, LUC+ luminescence intensity (L_{LUC+}) and PtRLUC luminescence intensity (L_{PtRLUC}) were calculated from green luminescence intensity (L_g) and red luminescence intensity (L_r) by using the following equation,

$$\begin{pmatrix} L_{LUC+} \\ L_{PtRLUC} \end{pmatrix} = \begin{pmatrix} 2.11 & -0.374 \\ -0.741 & 4.04 \end{pmatrix} \begin{pmatrix} L_g \\ L_r \end{pmatrix}.$$

By the fast Fourier transform non-linear least squares method (FFT-NLLS), the RAEs of bioluminescence traces were estimated using data in the time range 24-96 h.

The RAEs of bioluminescence traces were estimated by the fast Fourier transform non-linear least squares method (FFT-NLLS) as described previously (Muranaka and Oyama, 2016), using data in the time range 24-96 h. Peak times of bioluminescence traces were estimated by a local quadratic curve fitting (Muranaka and Oyama, 2016). Time-series data were smoothed with the 12-hour moving average, and peak positions were roughly identified as local maxima. Precise positions of peaks were estimated by a local quadratic curve fitting using the original time series data. The width of the local fitting area was set to 9 hours.

Acknowledgements

We thank Dr. Masaaki Morikawa for *Lemna minor* 5512. This work was supported in part by the Japan Society for the Promotion of Science KAKENHI (Grant numbers 25650098, 17KT0022, and 19H03245), the Japan Science and Technology Agency (JST) ALCA to T. O., and KAKENHI (Grant numbers 20K06342) to S. I., and KAKENHI (Grant numbers 24-1530) to T. M..

References

Chhabra, G., Chaudhary, D., Sainger, M. and Jaiwal, P.K. (2011) Genetic transformation of Indian isolate of *Lemna minor* mediated by *Agrobacterium tumefaciens* and recovery of transgenic plants. *Physiol. Mol. Biol. Plants*, **17**, 129–136.

Christensen, A.H., Sharrock, R.A. and Quail, P.H. (1992) Maize polyubiquitin genes: structure, thermal perturbation of expression and transcript splicing, and promoter activity following transfer to protoplasts by electroporation. *Plant Mol. Biol.*, **18**, 675–689.

Covington, M.F., Maloof, J.N., Straume, M., Kay, S.A. and Harmer, S.L. (2008) Global transcriptome analysis reveals circadian regulation of key pathways in plant growth and development. *Genome Biol.*, **9**, R130.

Dodd, A.N., Kusakina, J., Hall, A., Gould, P.D. and Hanaoka, M. (2014) The circadian regulation of photosynthesis. *Photosynth. Res.*, **119**, 181–190.

Endo, M., Shimizu, H., Nohales, M.A., Araki, T. and Kay, S.A. (2014) Tissue-specific clocks in *Arabidopsis* show asymmetric coupling. *Nature*, **515**, 419–422.

Feeney, K.A., Hansen, L.L., Putker, M., et al. (2016) Daily magnesium fluxes regulate cellular timekeeping and energy balance. *Nature*, **532**, 375–379.

Fukuda, H., Nakamichi, N., Hisatsune, M., Murase, H. and Mizuno, T. (2007) Synchronization of plant circadian oscillators with a phase delay effect of the vein network. *Phys. Rev. Lett.*, **99**, 098102.

Fukuda, H., Ukai, K. and Oyama, T. (2012) Self-arrangement of cellular circadian rhythms through phase-resetting in plant roots. *Phys. Rev. E*, **86**, 041917.

Hall, A., Kozma-Bognár, L., Bastow, R.M., Nagy, F. and Millar, A.J. (2002) Distinct regulation of *CAB* and *PHYB* gene expression by similar circadian clocks. *Plant J.*, **32**, 529–537.

Hillman, W.S. (1961) The Lemnaceae, or duckweeds: A review of the descriptive and experimental literature. *Bot. Rev.*, **27**, 221–287.

Hillman, W.S. (1970) Carbon dioxide output as an index of circadian timing in *Lemna* photoperiodism. *Plant Physiol.*, **45**, 273–279.

Isoda, M. and Oyama, T. (2018) Use of a duckweed species, *Wolffiella hyalina*, for whole-plant observation of physiological behavior at the single-cell level. *Plant Biotechnol.*, **35**, 387–391.

Kærn, M., Elston, T.C., Blake, W.J. and Collins, J.J. (2005) Stochasticity in gene expression: from theories to phenotypes. *Nat. Rev. Genet.*, **6**, 451–464.

Kanesaka, Y., Okada, M., Ito, S. and Oyama, T. (2019) Monitoring single-cell bioluminescence of *Arabidopsis* leaves to quantitatively evaluate the efficiency of a transiently introduced CRISPR/Cas9 system targeting the circadian clock gene *ELF3*. *Plant Biotechnol.*, **36**, 187–193.

Kitayama, Y., Kondo, T., Nakahira, Y., Nishimura, H., Ohmiya, Y. and Oyama, T. (2004) An *in vivo* dual-reporter system of cyanobacteria using two railroad-worm luciferases with different color emissions. *Plant Cell Physiol.*, **45**, 109–113.

Kondo, T. (1983) Phase shifts of potassium uptake rhythm in *Lemna gibba* G3 due to light, dark or temperature pulses. *Plant Cell Physiol.*, **24**, 659–665.

Kondo, T. and Nakashima, H. (1979) Content of adenosine phosphate compounds in a Long-Day Duckweed, *Lemna gibba* G3, under different light and nutritional conditions. *Physiol. Plant.*, **45**, 357–362.

Kondo, T. and Tsudzuki, T. (1978) Rhythm in potassium uptake by a duckweed, *Lemna gibba* G3. *Plant Cell Physiol.*, **19**, 1465–1473.

Kwon, H., Enomoto, T., Shimogawara, M., Yasuda, K., Nakajima, Y. and Ohmiya, Y. (2010) Bioluminescence imaging of dual gene expression at the single-cell level. *BioTechniques*, **48**, 460–462.

Les, D.H., Landolt, E. and Crawford, D.J. (1997) Systematics of the *Lemnaceae* (duckweeds): Inferences from micromolecular and morphological data. *Plant Syst. Evol.*, **204**, 161–177.

Linde, A.-M., Eklund, D.M., Kubota, A., et al. (2017) Early evolution of the land plant circadian clock. *New Phytol.*, **216**, 576–590.

Masuda, K., Kitaoka, R., Ukai, K., Tokuda, I.T. and Fukuda, H. (2017) Multicellularity enriches the entrainment of Arabidopsis circadian clock. *Sci. Adv.*, **3**, e1700808.

McClung, C.R. (2013) Beyond *Arabidopsis*: The circadian clock in non-model plant species. *Semin. Cell Dev. Biol.*, **24**, 430–436.

McClung, C.R. (2019) The plant circadian oscillator. *Biology*, **8**, 14.

Michael, T.P. and McClung, C.R. (2002) Phase-specific circadian clock regulatory elements in *Arabidopsis*. *Plant Physiol.*, **130**, 627–638.

Michael, T.P., Mockler, T.C., Breton, G., et al. (2008) Network discovery pipeline elucidates conserved time-of-day–specific cis-regulatory modules. *PLOS Genet.*, **4**, e14.

Millar, A.J., Short, S.R., Chua, N.H. and Kay, S.A. (1992) A novel circadian phenotype based on firefly luciferase expression in transgenic plants. *Plant Cell*, **4**, 1075–1087.

Miwa, K., Serikawa, M., Suzuki, S., Kondo, T. and Oyama, T. (2006) Conserved expression profiles of circadian clock-related genes in two *Lemna* species showing long-day and short-day photoperiodic flowering responses. *Plant Cell Physiol.*, **47**, 601–612.

Miyata, H. and Yamamoto, Y. (1969) Rhythms in respiratory metabolism of *Lemna gibba* G3 under continuous illumination. *Plant Cell Physiol.*, **10**, 875–889.

Muranaka, T., Kubota, S. and Oyama, T. (2013) A single-cell bioluminescence imaging system for monitoring cellular gene expression in a plant body. *Plant Cell Physiol.*, **54**, 2085–2093.

Muranaka, T., Okada, M., Yomo, J., Kubota, S. and Oyama, T. (2015) Characterisation of circadian rhythms of various duckweeds. *Plant Biol.*, **17**, 66–74.

Muranaka, T. and Oyama, T. (2020) Application of single-cell bioluminescent imaging to monitor circadian rhythms of individual plant cells. In *Bioluminescent Imaging: Methods and Protocols* (Ripp, S., eds). Methods in Molecular Biology. New York, NY: Springer US, pp. 231–242.

Muranaka, T. and Oyama, T. (2016) Heterogeneity of cellular circadian clocks in intact plants and its correction under light-dark cycles. *Sci. Adv.*, **2**, e1600500.

Muranaka, T. and Oyama, T. (2018) Monitoring circadian rhythms of individual cells in plants. *J. Plant Res.*, **131**, 15–21.

Nagel, D.H. and Kay, S.A. (2012) Complexity in the wiring and regulation of plant circadian networks. *Curr. Biol.*, **22**, R648–R657.

Nakajima, Y., Ikeda, M., Kimura, T., Honma, S., Ohmiya, Y. and Honma, K. (2004) Bidirectional role of orphan nuclear receptor RORα in clock gene transcriptions demonstrated by a novel reporter assay system. *FEBS Lett.*, **565**, 122–126.

Nakajima, Y., Kimura, T., Sugata, K., Enomoto, T., Asakawa, A., Kubota, H., Ikeda, M. and Ohmiya, Y. (2005) Multicolor luciferase assay system: one-step monitoring of multiple gene expressions with a single substrate. *BioTechniques*, **38**, 891–894.

Nakamichi, N., Ito, S., Oyama, T., Yamashino, T., Kondo, T. and Mizuno, T. (2004) Characterization of plant circadian rhythms by employing *Arabidopsis* cultured cells with bioluminescence reporters. *Plant Cell Physiol.*, **45**, 57–67.

Nishide, S., Honma, S. and Honma, K. (2018) Two coupled circadian oscillations regulate *Bmal1-ELuc* and *Per2-SLR2* expression in the mouse suprachiasmatic nucleus. *Sci. Rep.*, **8**, 14765.

Nishiguchi, T., Yamada, T., Nasu, Y., Ito, M., Yoshimura, H. and Ozawa, T. (2015) Development of red-shifted mutants derived from luciferase of Brazilian click beetle *Pyrearinus termitilluminans*. *J. Biomed. Opt.*, **20**, 101205.

Ogura, R., Matsuo, N., Wako, N., Tanaka, T., Ono, S. and Hiratsuka, K. (2005) Multi-color luciferases as reporters for monitoring transient gene expression in higher plants. *Plant Biotechnol.*, **22**, 151–155.

Okada, M., Muranaka, T., Ito, S. and Oyama, T. (2017) Synchrony of plant cellular circadian clocks with heterogeneous properties under light/dark cycles. *Sci. Rep.*, **7**, 317.

Plautz, J.D., Straume, M., Stanewsky, R., Jamison, C.F., Brandes, C., Dowse, H.B., Hall, J.C. and Kay, S.A. (1997) Quantitative analysis of drosophila period gene transcription in living animals. *J. Biol. Rhythms*, **12**, 204–217.

Serikawa, M., Miwa, K., Kondo, T. and Oyama, T. (2008) Functional conservation of clock-related genes in flowering plants: Overexpression and RNA interference analyses of the circadian rhythm in the monocotyledon *Lemna gibba*. *Plant Physiol.*, **146**, 1952–1963.

Stomp, A.-M. (2005) The duckweeds: A valuable plant for biomanufacturing. In *Biotechnology Annual Review*. Elsevier, pp. 69–99.

Takahashi, N., Hirata, Y., Aihara, K. and Mas, P. (2015) A herarchical multi-oscillator network orchestrates the *Arabidopsis* circadian system. *Cell*, **163**, 148–159.

Thain, S.C., Hall, A. and Millar, A.J. (2000) Functional independence of circadian clocks that regulate plant gene expression. *Curr. Biol.*, **10**, 951–956.

Thain, S.C., Murtas, G., Lynn, J.R., McGrath, R.B. and Millar, A.J. (2002) The circadian clock that controls gene expression in *Arabidopsis* is tissue specific. *Plant Physiol.*, **130**, 102–110.

Van Hoeck, A., Horemans, N., Monsieurs, P., Cao, H.X., Vandenhove, H. and Blust, R. (2015) The first draft genome of the aquatic model plant *Lemna minor* opens the route for future stress physiology research and biotechnological applications. *Biotechnol. Biofuels*, **8**, 188.

Van Leeuwen, W., Hagendoorn, M.J.M., Ruttink, T., Van Poecke, R., Van Der Plas, L.H.W. and Van Der Krol, A.R. (2000) The use of the luciferase reporter system for *in planta* gene expression studies. *Plant Mol. Biol. Report.*, **18**, 143–144.

Viviani, V.R. (2002) The origin, diversity, and structure function relationships of insect luciferases. *Cell. Mol. Life Sci.*, **59**, 1833–1850.

Wang, Z.-Y. and Tobin, E.M. (1998) Constitutive expression of the CIRCADIAN CLOCK ASSOCIATED 1 (CCA1) gene disrupts circadian rhythms and suppresses its own expression. *Cell*, **93**, 1207–1217.

Wenden, B., Toner, D.L.K., Hodge, S.K., Grima, R. and Millar, A.J. (2012) Spontaneous spatiotemporal waves of gene expression from biological clocks in the leaf. *Proc. Natl. Acad. Sci.*, **109**, 6757–6762.

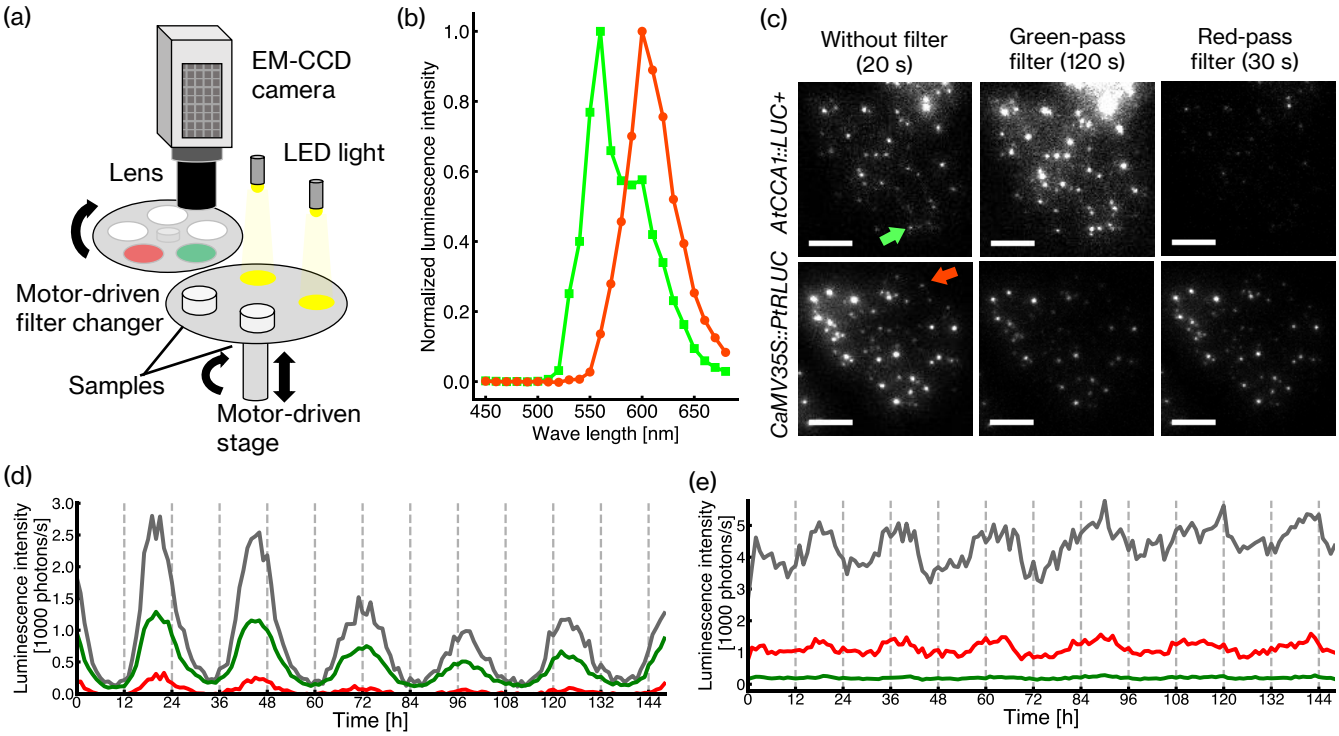

Figure 1. Measurement of bioluminescence of LUC+ and PtRLUC in *Lemna minor*

(a) Schematic drawing of the imaging device for the dual-color bioluminescence monitoring system. Sample dishes containing duckweed plants are set on a motor-driven stage. The stage rotates to exchange positions of a sample underneath the lens of an EM-CCD camera or an end of optic fibers guiding LED light. A motor-driven filter changer is set between the sample and the lens. The focus of an image for the sample is adjusted by a z-axis motor. (b) Luminescence spectra of LUC+ and PtRLUC expressed in duckweed cells. Luminescence emission of *L. minor* transfected with *CaMV35S::LUC+* or *CaMV35S::PtRLUC* by particle bombardment was filtered by a series of optical band-pass filters with a narrow band width (half width 10 nm) (Asahi Spectra), and the intensity of a filtered luminescence was obtained from the image of a luminous frond captured by the EM-CCD camera. Intensities normalized to the maximum are plotted. (c) Images of luminous spots in a frond of *L. minor* transfected with *AtCCA1::LUC+* (upper row) or *CaMV35S::PtRLUC* (lower row). A luminescence image of a frond without filter (left), and that of the same area filtered with a green-pass filter (490–570 nm) (middle) or with a red-pass filter (610–650 nm) (right) are shown. Exposure times for each filter condition are represented in parentheses. (d, e) Time series data of luminescence intensities of a luminous spot for *AtCCA1::LUC+* (d) and *CaMV35S::PtRLUC* (e) in each filter condition. Luminescence images for each filter condition were captured every 1 h. Luminescent intensities of the luminous spot pointed out in (c) by arrows are plotted (gray for without filter, green for green-pass filter, red for red-pass filter). The illumination conditions for the duckweed plant during luminescence monitoring was constant light. Images in (c) were captured at time 0 in (d) and (e). Bars represent 1 mm.

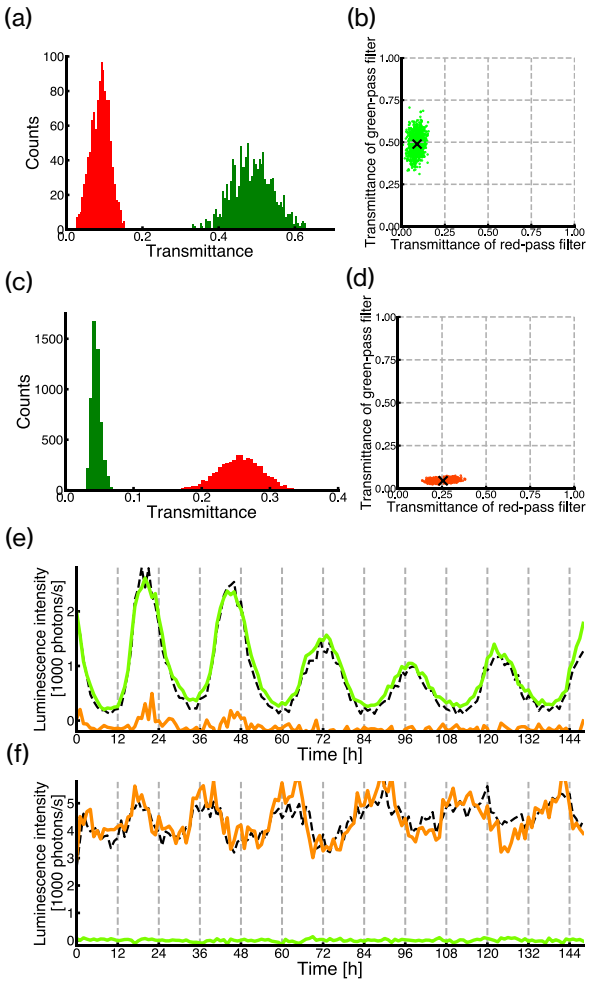

Figure 2. Estimation of luminescent intensities of LUC+ or PtRLUC by using intensities of filtered luminescence.

Time series data of luminescent intensities obtained in the same experiments as Figure 1c-e were used. 28 (LUC+) and 38 (PtRLUC) luminous spots with 149 time-lapse data (149 h) were calculated for transmittance. Those data including one or more pixels with saturated signal for either filtered luminescence in the spot area were excluded. (a, b) Histograms for transmittance of LUC+ (a) and PtRLUC (b) for green-pass (green bars) and red-pass filter (red bars). Data with unfiltered luminescent intensities (L) more than 1000 photons/s are counted (total 1129 spots for LUC+, 5354 spots for PtRLUC). The bin size is 0.05. (c, d) Scatter plots of transmittance for green-pass filter versus those for red-pass filter [(c) for LUC+, (d) for PtRLUC]. Transmittance for data with unfiltered luminescent intensities (L) more than 1000 photons/s are plotted. The cross mark shows the average transmittance. (e, f) Reconstruction of time series data of luminescence intensities of a luminous spot for *AtCCA1::LUC+* (e) and *CaMV35S::PtRLUC* (f). Luminescence of LUC+ (green line) and PtRLUC (red line) were reconstructed using time series data of filtered luminescence intensities that are represented in Figure 1d and 1e. A dotted line in each graph represents original time series data of unfiltered luminescent intensities.

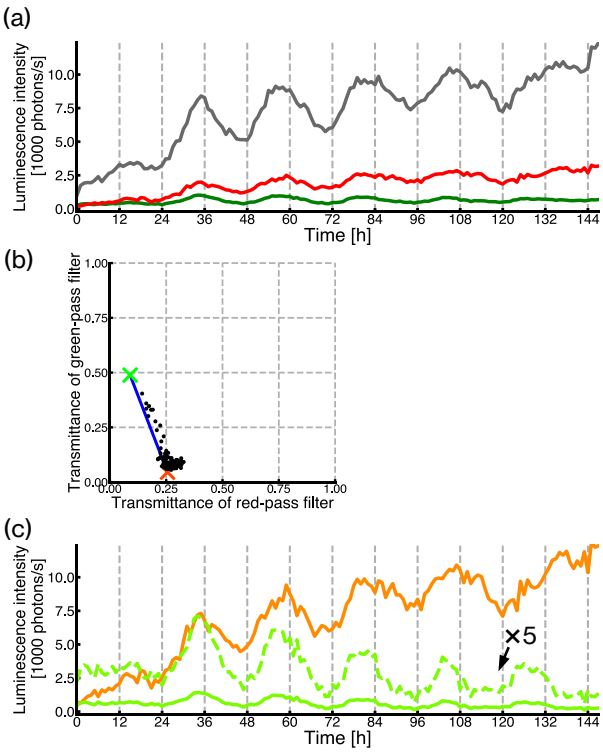

Figure 3. Reconstruction of luminescence intensities for *AtCCA1::LUC+* and *CaMV35S::PtRLUC* of a co-transfected cell.

Images of luminous spots in a frond of *L. minor* co-transfected with *AtCCA1::LUC+* and *CaMV35S::PtRLUC* were captured and analyzed data for a luminous spot with 149 time-lapse data (149 h) was shown. Growth, illumination, and monitoring conditions were the same as Figure 1de. (a) Time series data of luminescence intensities of a luminous cell in each filter condition. Luminescence intensities of the luminous spot are plotted (gray for without filter (L), green for green-pass filter (L_g), red for red-pass filter (L_r). (b) A scatter plot of transmittance for green-pass filter versus those for red-pass filter. Black dots represent the transmittance. Cross marks show the average transmittance for *AtCCA1::LUC+* (green, Figure 2c) or *CaMV35S::PtRLUC* (red, Figure 2d). Those data satisfying the formula: $L_{LUC+} + L_{PtRLUC} = L$, are plotted on the blue line segment. (c) Reconstructed time series data of luminescence intensities for *AtCCA1::LUC+* (light green line) and *CaMV35S::PtRLUC* (orange line). A dotted light green line in each graph represents five-fold magnification of LUC+.

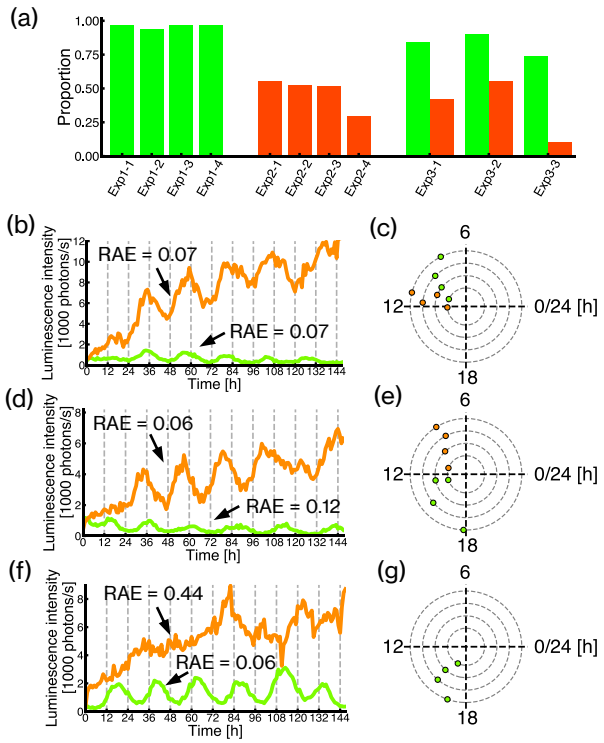

Figure 4 Quantitative analysis of cellular rhythms for *AtCCA1::LUC+* and *CaMV35S::PtRLUC* of co-transfected cells.

(a) Circadian rhythmicity of cellular bioluminescence activities of *AtCCA1::LUC+* and *CaMV35S::PtRLUC.* Red- and green bars represent proportions of cells showing bioluminescence traces with circadian rhythms (RAE < 0.2) in single transfection experiments *for AtCCA1::LUC+* (Exp.1-1 ~ 1-4) and *CaMV35S::PtRLUC* (Exp.2-1 ~ 2-3), and co-transfection experiments for both reporters (Exp.3-1 ~ 3-3). (b, d, f) Examples of reconstructed timeseries data of luminescence intensities for *AtCCA1::LUC+* (light green line) and *CaMV35S::PtRLUC* (orange line) in a co-transfection experiment (Exp. No.3-1). The RAE value for each bioluminescence trace is represented. (c, e, g) Time of peaks of individual cellular bioluminescence rhythms of *AtCCA1::LUC+* (light green) and *CaMV35S::PtRLUC* (orange). Peak time(s) shown in Day 2 (24-48 h) is plotted on the innermost circle and those in Day3 (48-72 h), Day 4 (72-96 h) and Day 5 (96–120 h) are plotted on the second, third and fourth circles, respectively. Peak times of the bioluminescence rhythms (RAE < 0.2) in (b), (d) and (f) are represented in (c), (e) and (g), respectively.

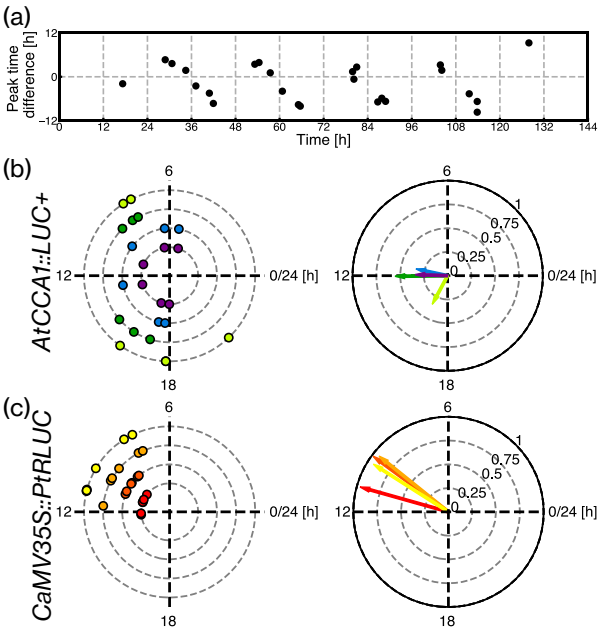

Figure 5. Characterization of phase relationship of cellular bioluminescence rhythms of *AtCCA1::LUC+* and *CaMV35S::PtRLUC* in the co-transfection experiment

(a) Analysis of peak time differences between *CaMV35S::PtRLUC-* and *AtCCA1::LUC+* rhythms in Exp. 3-1. Peak time differences of bioluminescence rhythms between the two reporters for cells showing circadian rhythms (RAE < 0.2) in both reporters (total six cells in this experiment) are plotted. Peak time differences are calculated by the subtraction of peak time of *AtCCA1::LUC+* rhythm from that of *CaMV35S::PtRLUC* rhythm, and those ranging from -12 to 12 h are plotted against each peak time of *AtCCA1::LUC+* rhythm. (b, c) Analysis of peak times of cellular bioluminescence rhythms in Exp. 3-1. Peak times of the six cells are plotted for *AtCCA1::LUC+* (b) and *CaMV35S::PtRLUC* (c) at left. Data display and plotting are the same as in (Figure 4c, 4e, 4g) except dots are color-coded by the day. At right, the vector sum of the plot for each day (the diameter is normalized as 1) is indicated by the arrow of the same color-code. The angle and the magnitude of a vector represents the average peak time and the degree of synchronicity, respectively.

Supporting Information for

Detection of uncoupled circadian rhythms in individual cells of *Lemna minor* by using a dual-color bioluminescence monitoring system

Emiri Watanabe, Minako Isoda, Tomoaki Muranaka, Shogo Ito, and Tokitaka Oyama

Contents:

Figure S1. Transfection of *Lemna minor* with reporters by the particle bombardment.
Figure S2. Time-series data at a whole plant level of *L. minor* transfected with *CaMV35S::LUC+* or *CaMV35S::PtRLUC.*
Figure S3. Scatter plots of transmittance versus luminescence intensities without filter in single reporter transfection experiments.
Figure S4. Comparison of transmittance of filters between *AtCCA1::LUC+* and *CaMV35S::LUC+*.
Figure S5. Schematic drawing for the calculation of luminescence intensities of LUC+ and PtRLUC.
Figure S6. Reconstruction of time series of luminescence intensities of luminous spots for *AtCCA1::LUC+* in a single transfection experiment.
Figure S7. Reconstruction of time series of luminescence intensities of luminous spots for *CaMV35S::PtRLUC* in a single transfection experiment.
Figure S8. Reconstruction of time series of luminescence intensities of luminous spots in a co-transfection experiment.
Figure S9. Flow diagram for the analysis for *AtCCA1::LUC+* and *CaMV35S::LUC+* co-transfection experiments.
Figure S10. Examples of bioluminescence traces with various RAE values in single transfection experiments.
Figure S11. Characterization of phase relationship of cellular bioluminescence rhythms of *AtCCA1::LUC+* and *CaMV35S::PtRLUC* in the co-transfection experiment, Exp3-2.
Figure S12. A scatter plot of free running period (FRP) between *AtCCA1::LUC+* rhythm and *CaMV35S::PtRLUC* rhythm in co-transfection experiments.
Table S1. Summary of the quantitative analysis of cellular bioluminescence rhythms.

Legends for Supporting Information

Figure S1. Transfection of *Lemna minor* with reporters by the particle bombardment.
A bright-field image of *L. minor* transfected with the bioluminescence reporter *CaMV35S::PtRLUC* (a, left), and a luminescence image captured 24 h after particle bombardment (a, right). An epidermal cell (b, upper) and a mesophyll cell (b, lower) that were transfected with the fluorescence reporter gene *CaMV35S::GFP-h*. A bright-field image (b, left) and a fluorescence image (b, right) are shown. 1252 fluorescent cells in three independent experiments were observed and classified into epidermal- or mesophyll cells and their percentages are show in (c). Error bars represent the SD. Scale bars in (a) and (b) are 2 mm and 20 µm, respectively.

Figure S2. Time-series data at a whole plant level of *L. minor* transfected with *CaMV35S::LUC+* or *CaMV35S::PtRLUC.*
CaMV35S::LUC+ (a, c) or *CaMV35S::PtRLUC* (b, d) was introduced into *L. minor* by particle bombardment and those plants were monitored under constant light conditions by using the luminescence dish-monitoring system used photomultiplier tubes. Three samples for each condition were monitored. The experimental schedule is shown at the upper part of each graph. Black and open bars indicate dark and light, respectively. The timing of gene transfection is shown by an arrow.

Figure S3. Scatter plots of transmittance versus luminescence intensities without filter in single reporter transfection experiments.
Transmittance of LUC+ (a) and PtRLUC (b) for green-pass (green dots) and red-pass filter (red dots) are plotted against luminescence intensities without filter. Time-series data of luminescence intensities obtained in the same experiments as Figure 1c-e were used (Exp1-1 and Exp2-1 in Table S1). 28 (LUC+) and 38 (PtRLUC) luminous spots with 149 time-series data (149 h) were calculated for transmittance. Those data including one or more pixels with saturated signal for either filtered luminescence in the spot area were excluded and the total spot numbers are 4151 (LUC+) and 5558 (PtRLUC).

Figure S4. Comparison of transmittance of filters between *AtCCA1::LUC+* and *CaMV35S::LUC+*.
Transmittance for each datapoint in time series of luminescence intensities is plotted for *AtCCA1::LUC+* (Exp1-1 in Table S1, total 4151 spots) and that for luminous spots in snapshot images is plotted for *CaMV35S::LUC+* (total 2147 spots). (a) Transmittance of *AtCCA1::LUC+* (green dot), *CaMV35S::LUC+* (blue dot) for green-pass filter is plotted against luminescence intensities without filter. (b) Transmittance of *AtCCA1::LUC+* (red dot), *CaMV35S::LUC+* (orange dot) for red-pass filter are plotted against luminescence intensities without filter. The cross mark represents the median for each condition.

Figure S5. Schematic drawing for the calculation of luminescence intensities of LUC+ and PtRLUC.
(a) Transmittance values of green-pass filter and red-pass filter for LUC+ luminescence are represented as K_g^{LUC+} and K_r^{LUC+}, respectively. In the single transfection experiment, $L_g = K_g^{LUC+} \times L_{LUC+}$, where L_g is

luminescence transmitted through the green-pass filter and L_{LUC+} is LUC+ luminescence as mentioned in Methods. Similarly, $L_r = K_r^{LUC+} \times L_{LUC+}$. (b) Transmittance values of green-pass filter and red-pass filter for PtRLUC luminescence are represented as K_g^{PtRLUC} and K_r^{PtRLUC}, respectively. Similarly to (a), in the single transfection experiment, $L_g = K_g^{PtRLUC} \times L_{PtRLUC}$ and $L_r = K_r^{PtRLUC} \times L_{PtRLUC}$. (c) In the co-transfection experiment, $L_g = K_g^{LUC+} \times L_{LUC+} + K_g^{PtRLUC} \times L_{PtRLUC}$ and $L_r = K_r^{LUC+} \times L_{LUC+} + K_r^{PtRLUC} \times L_{PtRLUC}$. The luminescence intensities from the two luciferases in the co-transfection experiment are calculated with inverse matrix A^{-1} as in the box for calculation formula. In our experiments, we used matrix elements described in the box for representative values.

Figure S6. Reconstruction of time series of luminescence intensities of luminous spots for *AtCCA1::LUC+* in a single transfection experiment.

Luminescence of LUC+ (light green line) and PtRLUC (orange line) were reconstructed using time-series data of filtered luminescence intensities for each cell in Exp1-1 (Table S1). A dotted line in each graph represents original time series of unfiltered luminescence intensities. The arrows (Spot No. 10) show an example where the L_{LUC+}- and L_{PtRLUC} values are underestimated and overestimated, respectively.

Figure S7. Reconstruction of time series of luminescence intensities of luminous spots for *CaMV35S::PtRLUC* in a single transfection experiment.

Luminescence of LUC+ (light green line) and PtRLUC (orange line) were reconstructed using timeseries data of filtered luminescence intensities for each cell in Exp2-1 (Table S1). A dotted line in each graph represents original time series of unfiltered luminescence intensities. Spot No.2, 4, 5, 9, 17, 27, 28, 29, 34, 38 contain data points with saturated signals in luminescence measurement. Estimated luminescence of LUC+ is near the baseline and almost invisible in each graph.

Figure S8. Reconstruction of time series of luminescence intensities of luminous spots in a co-transfection experiment.

Luminescence of LUC+ (light green line) and PtRLUC (orange line) were reconstructed using time-series data of filtered luminescence intensities for each cell in Exp3-1 (Table S1). A dotted light green line in each graph represents five-fold magnification of LUC+. P and B in the graph represent analyzable spots and cells showing circadian rhythms of both reporters, respectively (refer Figure S9). Spot No.29 and spot No.34 showed a saturation of luminescence and these spots were excluded from reconstruction.

Figure S9. Flow diagram for the analysis for *AtCCA1::LUC+* and *CaMV35S::LUC+* co-transfection experiments.

(*) Luminous spots without overlapping each other are counted. (**) Luminous spots that include saturated pixels in the 6×6 spot area at two successive timepoints in the monitoring period (24 - 144 h) are removed. (***) Those spots with the following three criteria are selected as analyzable spots for the both reporters.

(1) Median of MA(L_{LUC+}) > 50 photons/s and median of MA(L_{PtRLUC}) > 500 photons/s.

(2) Median of MA(L_{LUC+}) < 5000 photons/s.

(3) The number of R(i) in the range 1/20 < R(i) < 1, is more than half of the total number of datapoints.

Definitions of each symbol in the criteria are as follows.

L_{LUC+}, L_{PtRLUC} at time i are defined as $L_{LUC+}(i)$, $L_{PtRLUC}(i)$. 24-hour moving average of X at time i ($MA[X, i]$) is defined as follows.

$MA[X, i] = 1/24 \times (X(\mathrm{i}) + ... + X(i+23))$

The luminescence ratio of LUC+ and PtRLUC at time i is defined as follows.

$\mathrm{R(i)} = MA[L_{LUC+}, i]/MA[L_{PtRLUC}, i]$

Dataset of time series $Y(i)$ is described as Y.

Figure S10. Examples of bioluminescence traces with various RAE values in single transfection experiments.

Reconstructed time series of 7 cells for LUC+ (light green, Exp1-1) and 10 cells for PtRLUC (orange, Exp2-1) are sorted by their RAE values. The RAE value is represented in each graph.

Figure S11. Characterization of phase relationship of cellular bioluminescence rhythms of *AtCCA1::LUC+* and *CaMV35S::PtRLUC* in the co-transfection experiment, Exp3-2.

(a) Reconstructed time series of LUC+ (light green line) and PtRLUC (orange line) for the nine cells showing circadian rhythms of both reporters in Exp3-2 (Table S1). The dotted vertical lines show the peak times of LUC+ (light green) and PtRLUC (orange). (b) Analysis of peak time differences between *CaMV35S::PtRLUC*- and *AtCCA1::LUC+* rhythms in Exp3-2. Peak time differences of bioluminescence rhythms between the two reporters for cells showing circadian rhythms (RAE < 0.2) in both reporters (total nine cells in this experiment) are plotted. Peak time differences are calculated by the subtraction of peak time of *AtCCA1::LUC+* rhythm from that of *CaMV35S::PtRLUC* rhythm, and those ranging from -12 to 12 h are plotted against each peak time of *AtCCA1::LUC+* rhythm. Peaks occurred in the range from 0 to 96 h are plotted because the circadian rhythmicity of *CaMV35S::PtRLUC* of most cells were lost after the range. (c, d) Analysis of peak times of cellular bioluminescence rhythms in Exp3-2. Peak times of the nine cells are plotted for *AtCCA1::LUC+* (c) and *CaMV35S::PtRLUC* (d) at left. Data display and plotting are the same as in Figure 5. Peak time(s) shown in Day 2 (24-48 h) is plotted on the innermost circle and those in Day3 (48-72 h) and Day 4 (72-96 h) are plotted on the second and third circles, respectively.

Figure S12. A scatter plot of free running period (FRP) between *AtCCA1::LUC+* rhythm and *CaMV35S::PtRLUC* rhythm in co-transfection experiments.

FRPs of the 21 cells in the co-transfection experiments (Table S1) are plotted. The same symbol (with the same color) represents cells in the same experiment.

Figure S1.

(a)

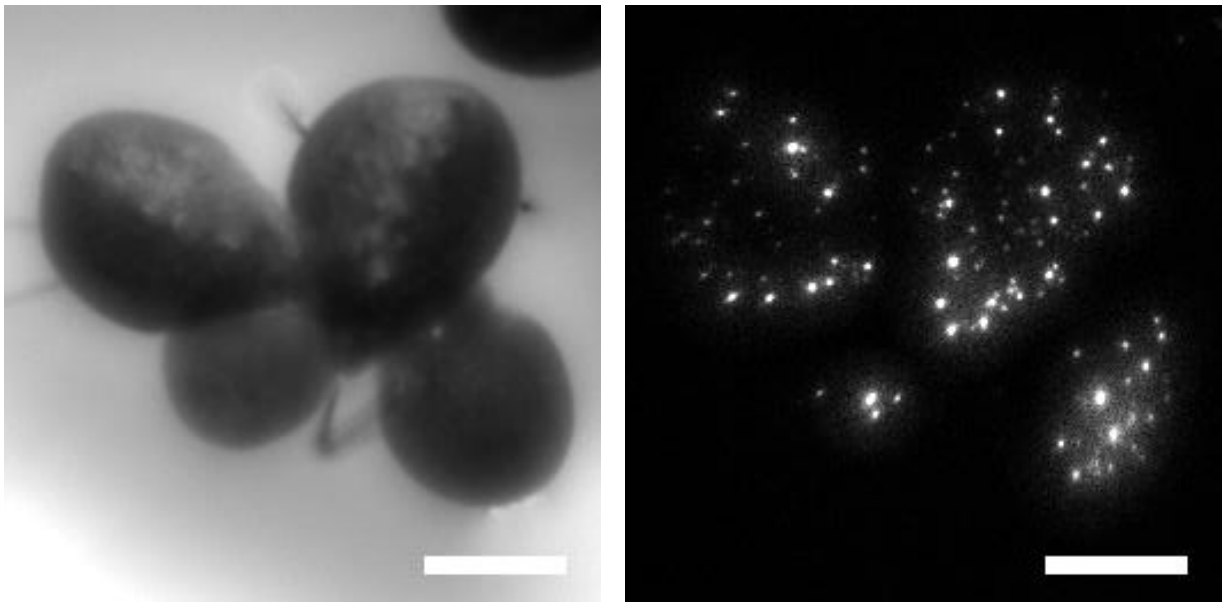

(b)

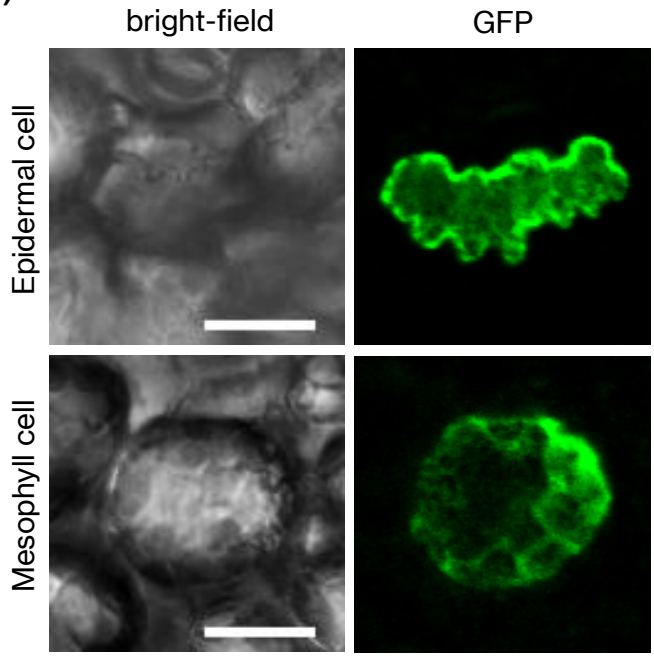

(c)

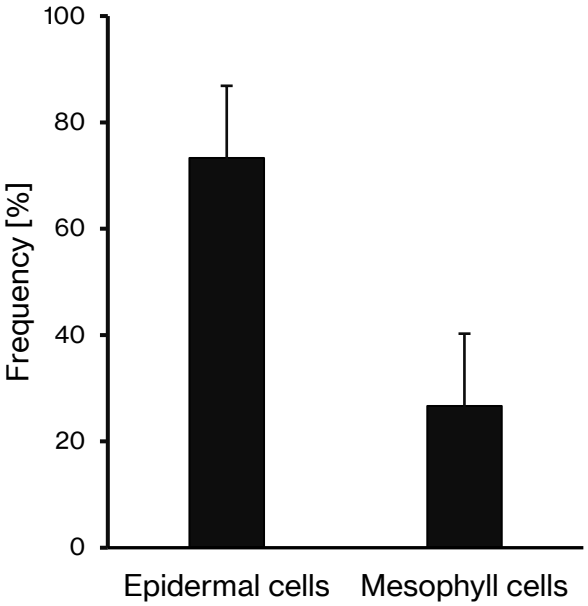

Figure S2.

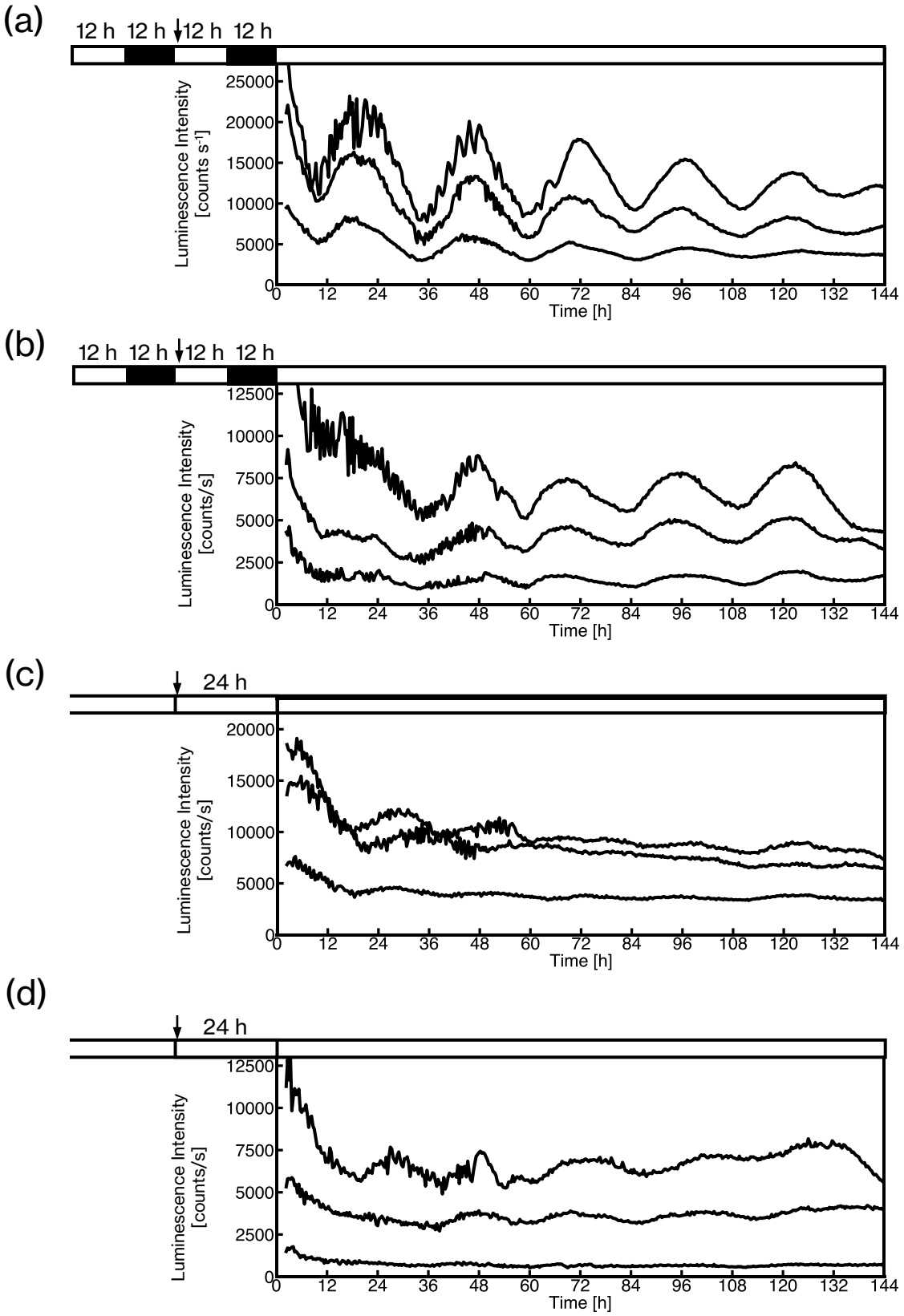
(a)
12 h 12 h 12 h 12 h
Luminescence Intensity [counts s-1]
25000
20000
15000
10000
5000
0
0 12 24 36 48 60 72 84 96 108 120 132 144
Time [h]
(b)
12 h 12 h 12 h 12 h
Luminescence Intensity [counts/s]
12500
10000
7500
5000
2500
0
0 12 24 36 48 60 72 84 96 108 120 132 144
Time [h]
(c)
24 h
Luminescence Intensity [counts/s]
20000
15000
10000
5000
0
0 12 24 36 48 60 72 84 96 108 120 132 144
Time [h]
(d)
24 h
Luminescence Intensity [counts/s]
12500
10000
7500
5000
2500
0
0 12 24 36 48 60 72 84 96 108 120 132 144
Time [h]

Figure S3.

(a)

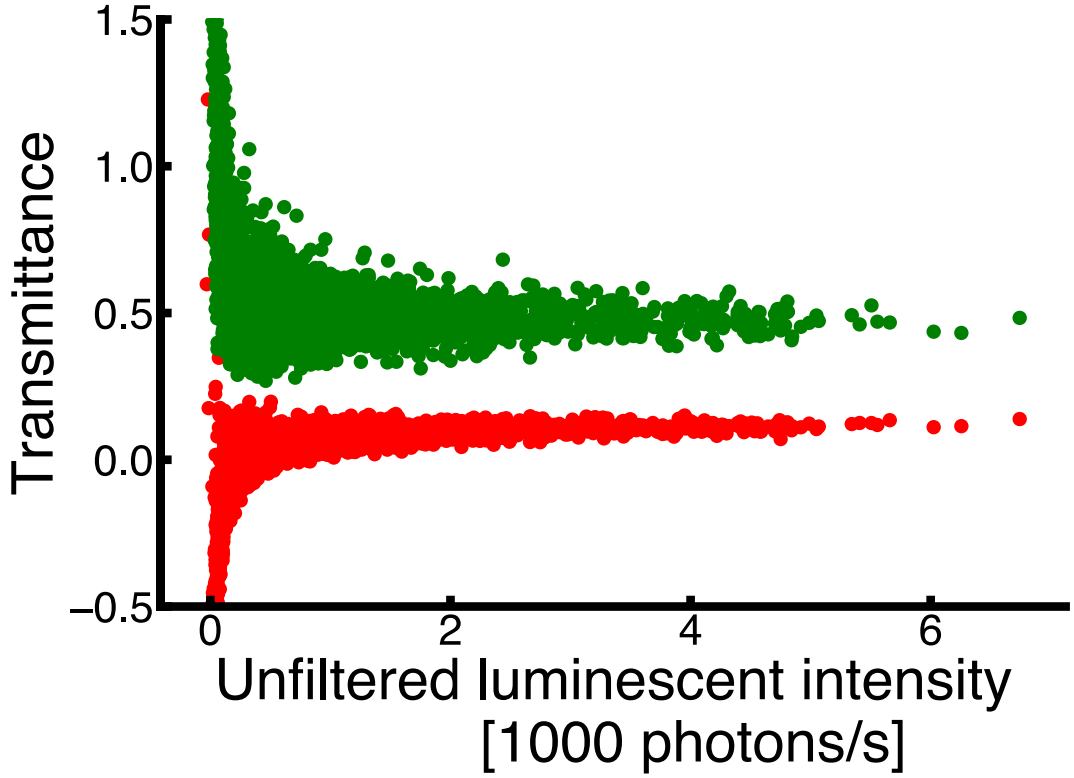
1.5
1.0
0.5
0.0
–0.5
Transmittance
0
2
4
6
Unfiltered luminescent intensity
[1000 photons/s]

(b)

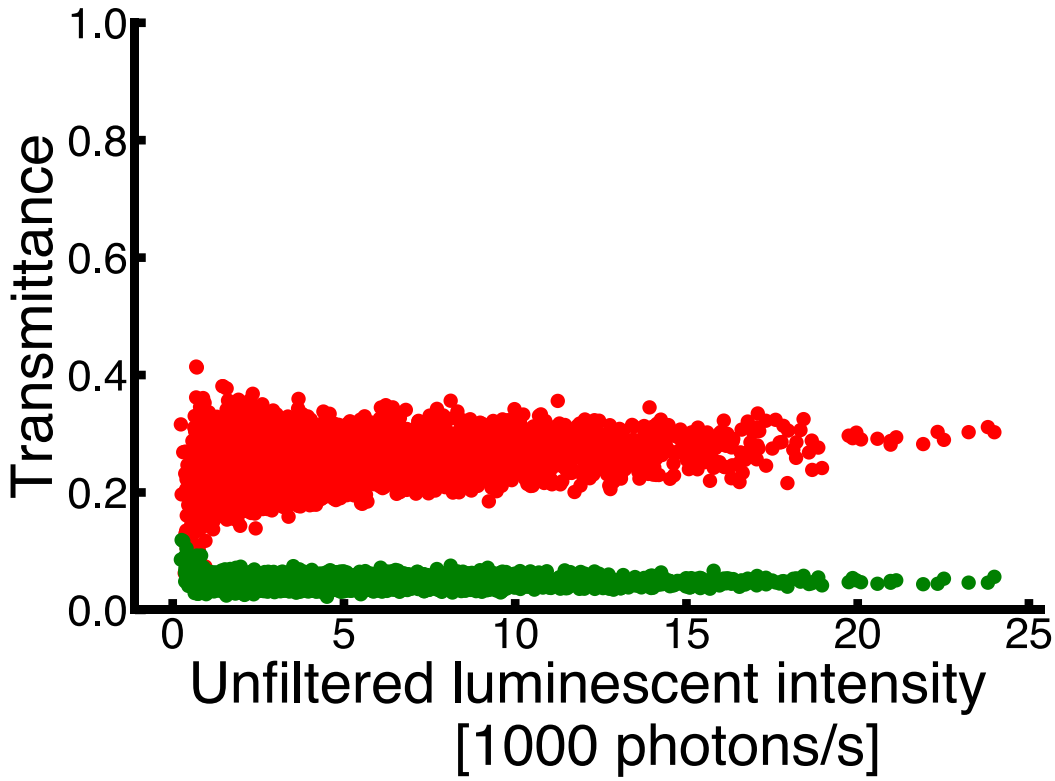
1.0
0.8
0.6
0.4
0.2
0.0
Transmittance
0
5
10
15
20
25
Unfiltered luminescent intensity
[1000 photons/s]

Figure S4.

(a)

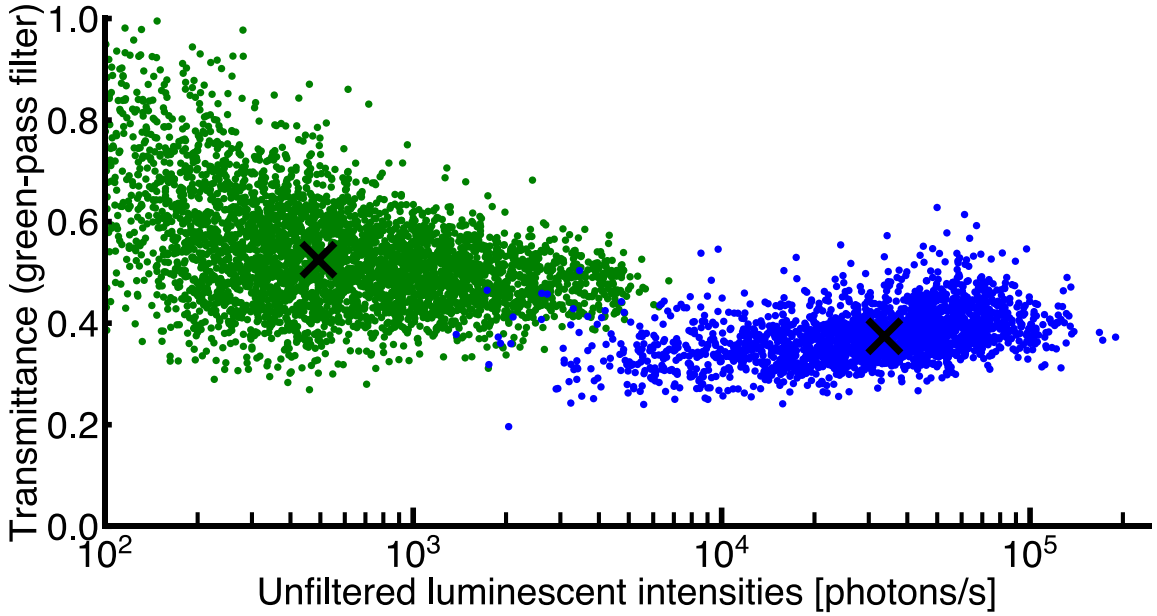
Transmittance (green-pass filter)
1.0
0.8
0.6
0.4
0.2
0.0
10^2
10^3
10^4
10^5
Unfiltered luminescent intensities [photons/s]

(b)

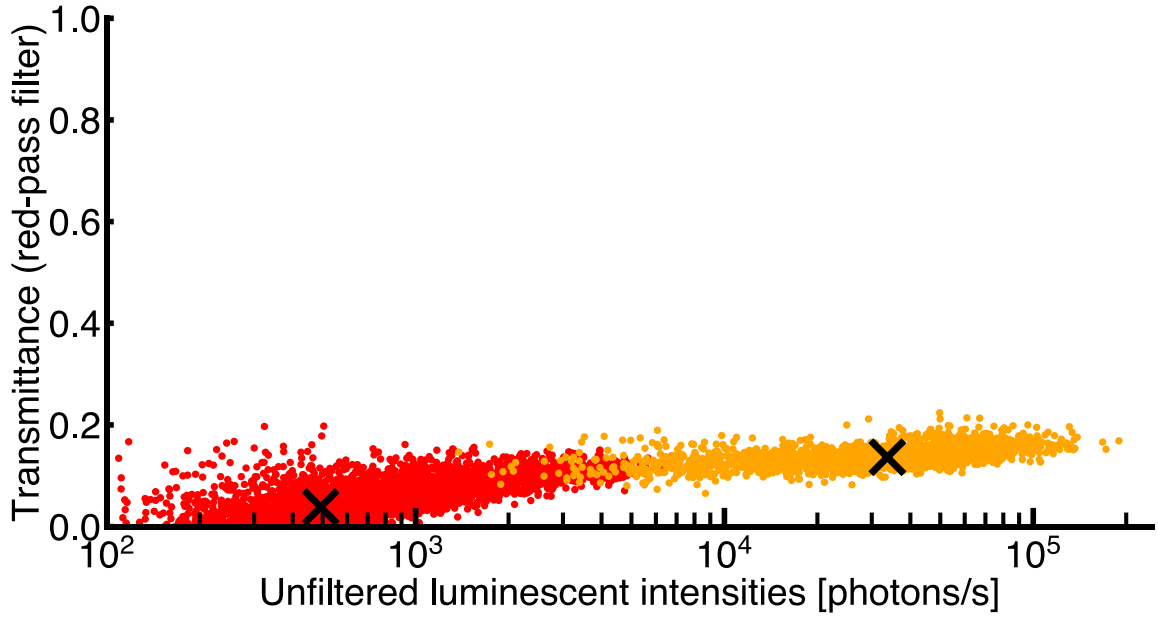
Transmittance (red-pass filter)
1.0
0.8
0.6
0.4
0.2
0.0
10^2
10^3
10^4
10^5
Unfiltered luminescent intensities [photons/s]

Figure S5.

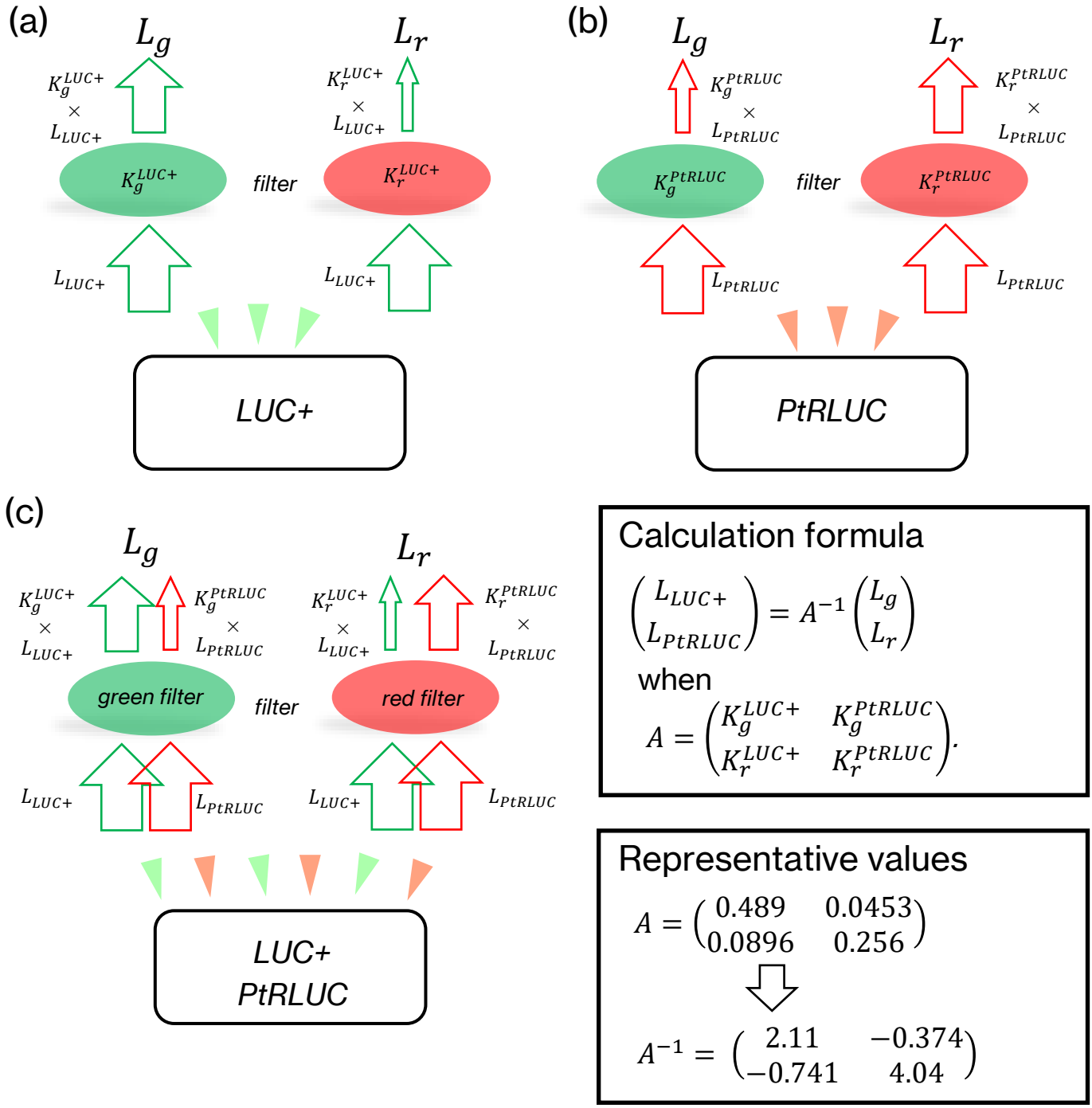

Calculation formula

$$\begin{pmatrix} L_{LUC+} \\ L_{PtRLUC} \end{pmatrix} = A^{-1} \begin{pmatrix} L_g \\ L_r \end{pmatrix}$$

when

$$A = \begin{pmatrix} K_g^{LUC+} & K_g^{PtRLUC} \\ K_r^{LUC+} & K_r^{PtRLUC} \end{pmatrix}.$$

Representative values

$$A = \begin{pmatrix} 0.489 & 0.0453 \\ 0.0896 & 0.256 \end{pmatrix}$$

$$\Downarrow$$

$$A^{-1} = \begin{pmatrix} 2.11 & -0.374 \\ -0.741 & 4.04 \end{pmatrix}$$

Figure S6.

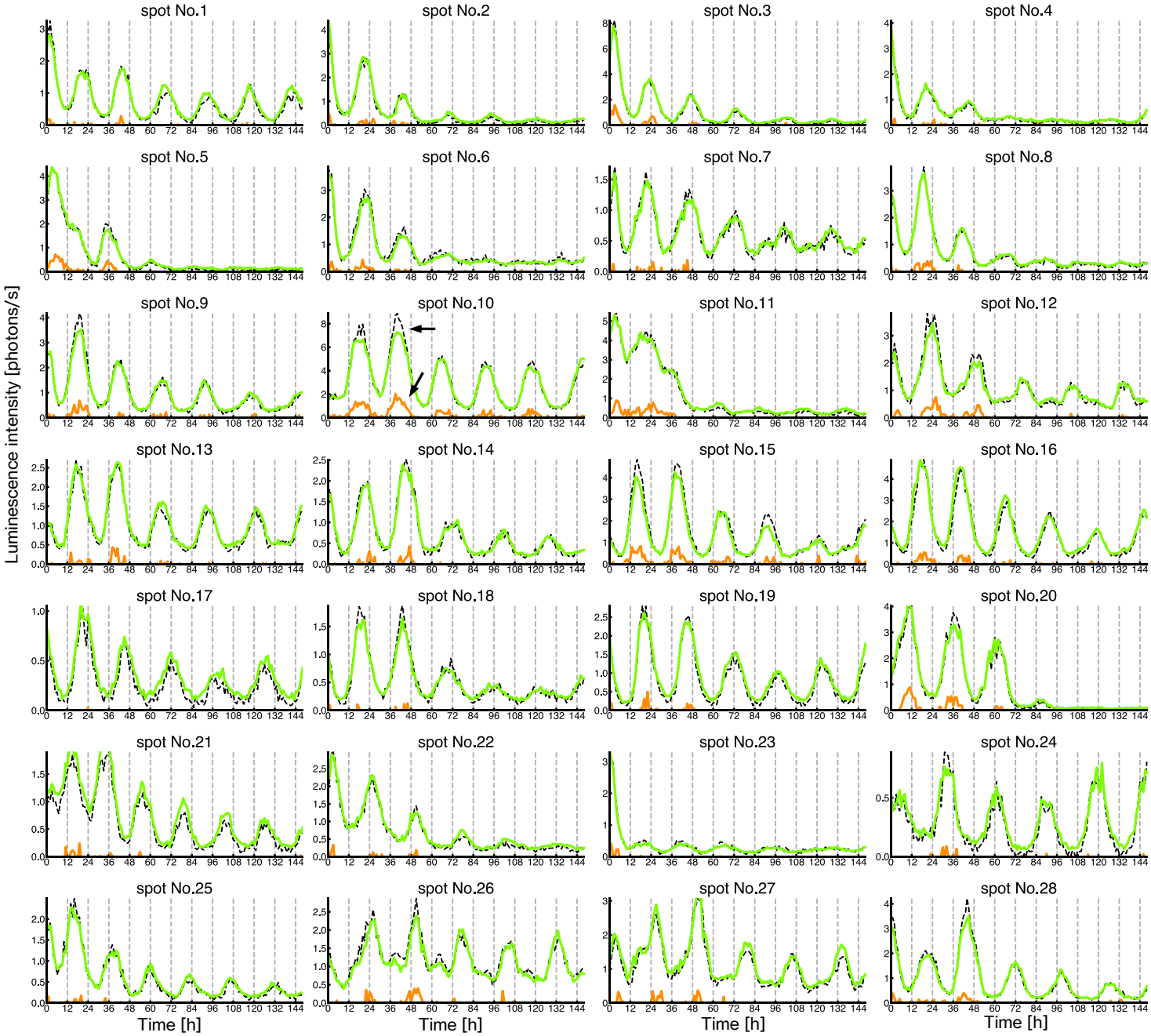
spot No.1
spot No.2
spot No.3
spot No.4
spot No.5
spot No.6
spot No.7
spot No.8
spot No.9
spot No.10
spot No.11
spot No.12
spot No.13
spot No.14
spot No.15
spot No.16
spot No.17
spot No.18
spot No.19
spot No.20
spot No.21
spot No.22
spot No.23
spot No.24
spot No.25
spot No.26
spot No.27
spot No.28
Luminescence intensity [photons/s]
Time [h]
Time [h]
Time [h]
Time [h]

Figure S7.

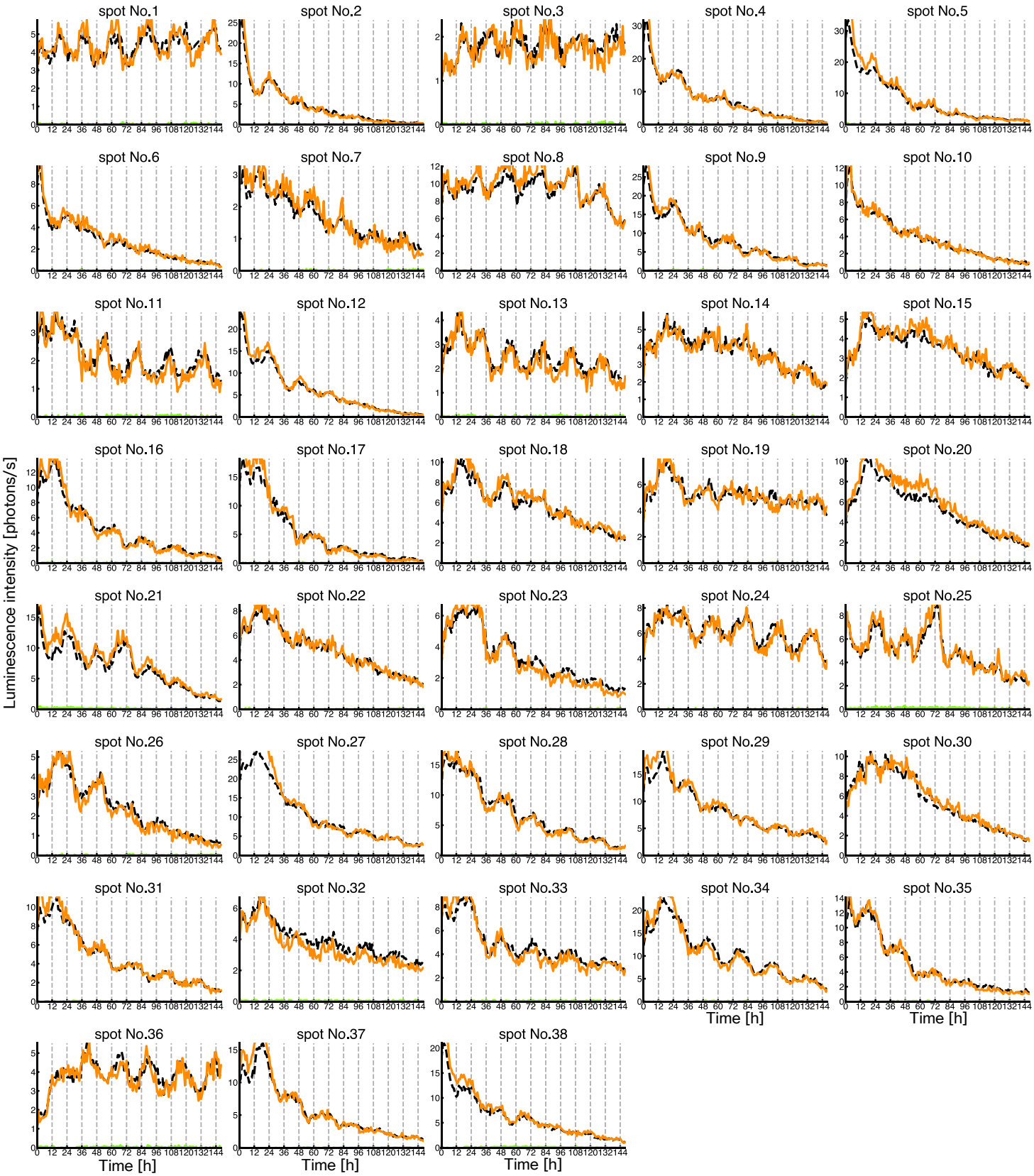
spot No.1
spot No.2
spot No.3
spot No.4
spot No.5
spot No.6
spot No.7
spot No.8
spot No.9
spot No.10
spot No.11
spot No.12
spot No.13
spot No.14
spot No.15
spot No.16
spot No.17
spot No.18
spot No.19
spot No.20
spot No.21
spot No.22
spot No.23
spot No.24
spot No.25
spot No.26
spot No.27
spot No.28
spot No.29
spot No.30
spot No.31
spot No.32
spot No.33
spot No.34
spot No.35
spot No.36
spot No.37
spot No.38
Luminescence intensity [photons/s]
Time [h]

Figure S8.

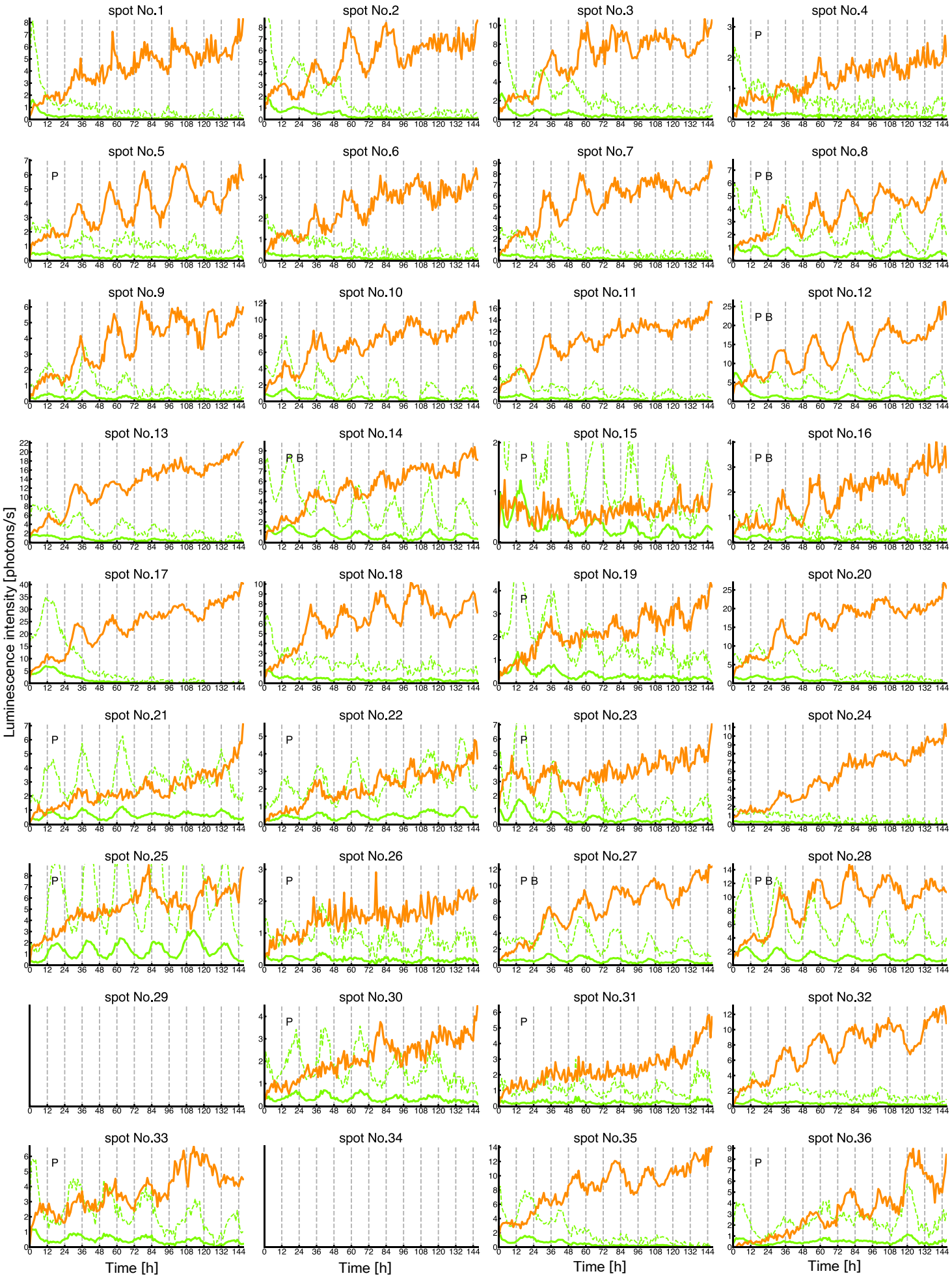
spot No.1
spot No.2
spot No.3
spot No.4
spot No.5
spot No.6
spot No.7
spot No.8
spot No.9
spot No.10
spot No.11
spot No.12
spot No.13
spot No.14
spot No.15
spot No.16
spot No.17
spot No.18
spot No.19
spot No.20
spot No.21
spot No.22
spot No.23
spot No.24
spot No.25
spot No.26
spot No.27
spot No.28
spot No.29
spot No.30
spot No.31
spot No.32
spot No.33
spot No.34
spot No.35
spot No.36
P
P B
Luminescence intensity [photons/s]
Time [h]

Figure S9.

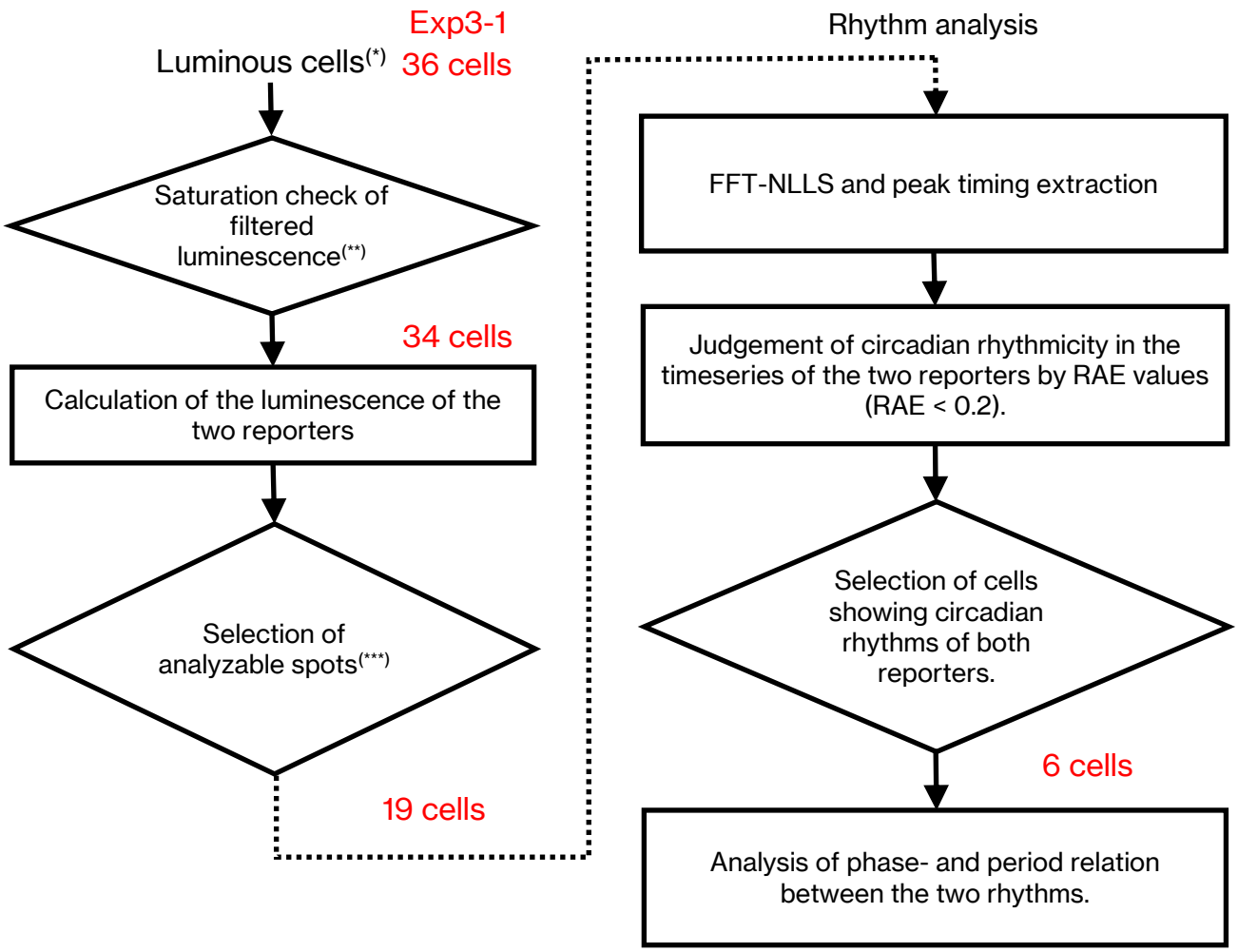
Exp3-1
Luminous cells(*)
36 cells
Saturation check of filtered luminescence(**)
34 cells
Calculation of the luminescence of the two reporters
Selection of analyzable spots(***)
19 cells
Rhythm analysis
FFT-NLLS and peak timing extraction
Judgement of circadian rhythmicity in the timeseries of the two reporters by RAE values (RAE < 0.2).
Selection of cells showing circadian rhythms of both reporters.
6 cells
Analysis of phase- and period relation between the two rhythms.

Figure S10.

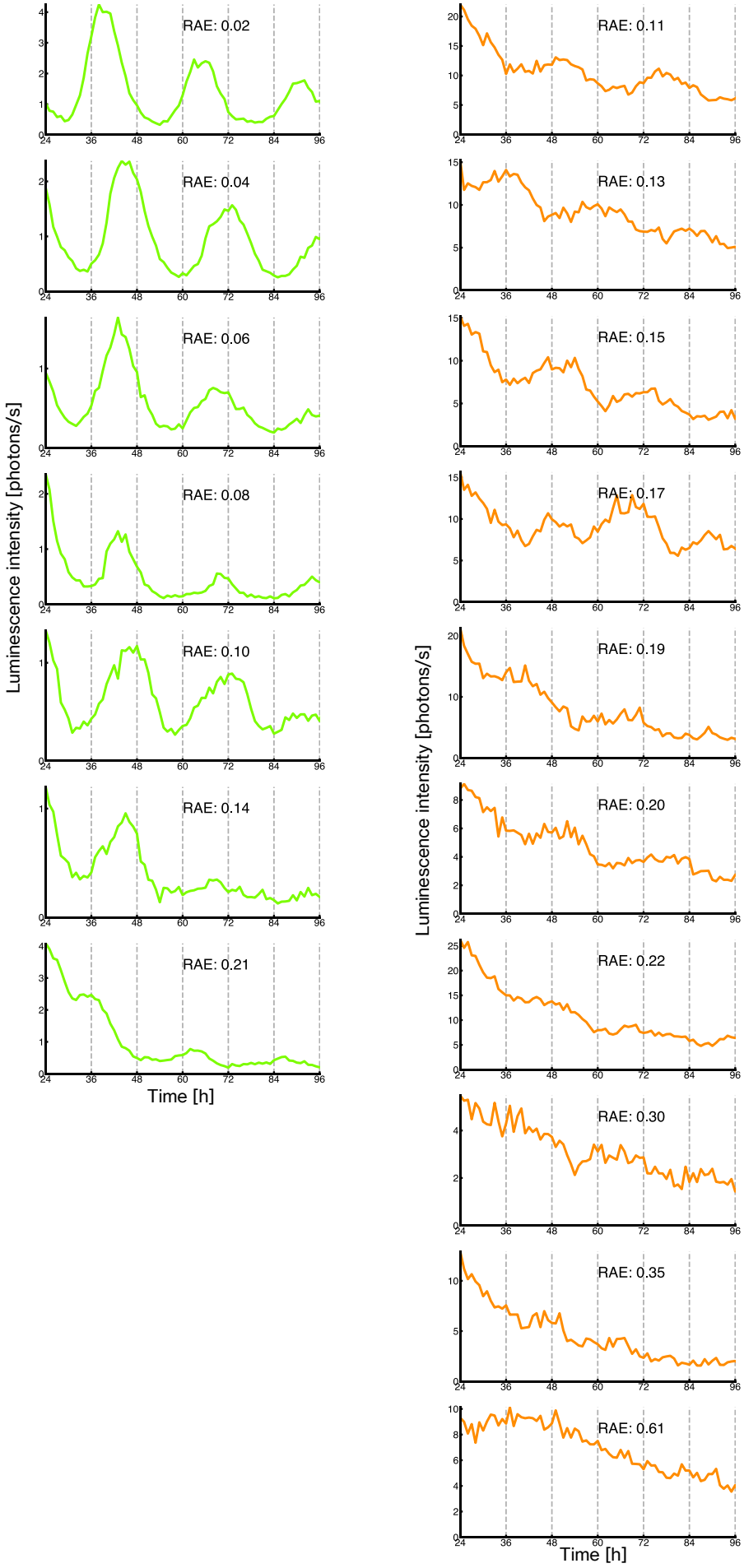
RAE: 0.02
RAE: 0.04
RAE: 0.06
RAE: 0.08
RAE: 0.10
RAE: 0.14
RAE: 0.21
RAE: 0.11
RAE: 0.13
RAE: 0.15
RAE: 0.17
RAE: 0.19
RAE: 0.20
RAE: 0.22
RAE: 0.30
RAE: 0.35
RAE: 0.61
Luminescence intensity [photons/s]
Time [h]

Figure S11.

(a)

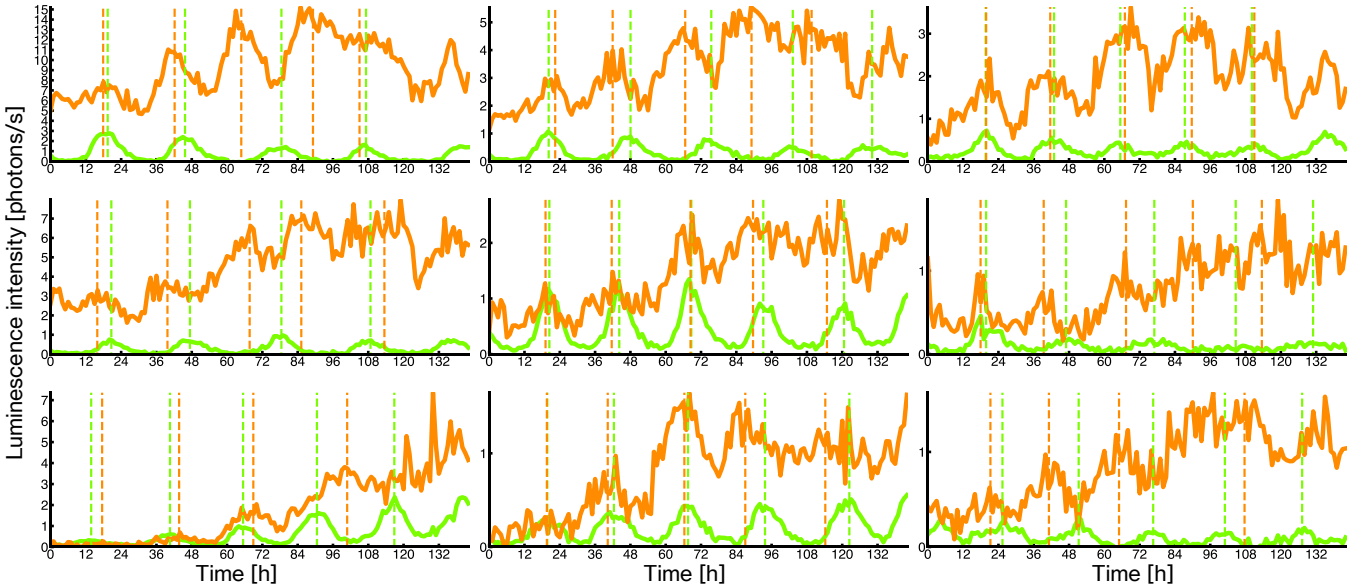

(b)

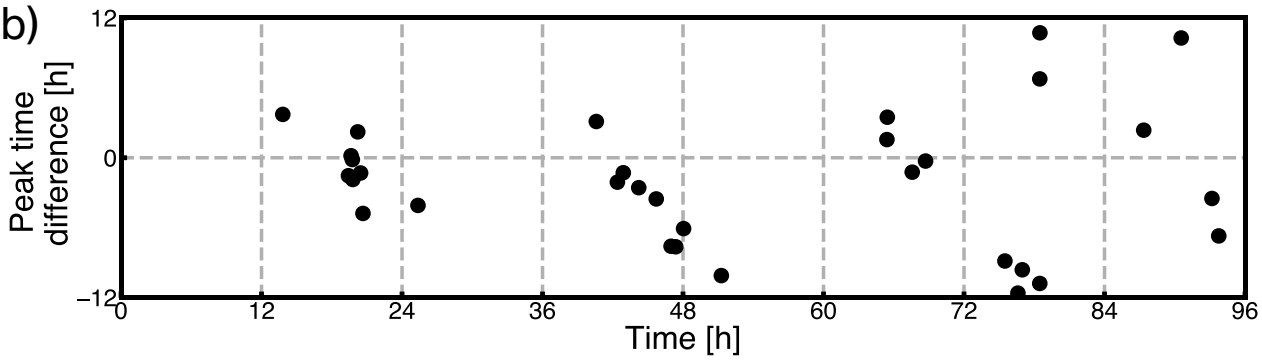

(c)

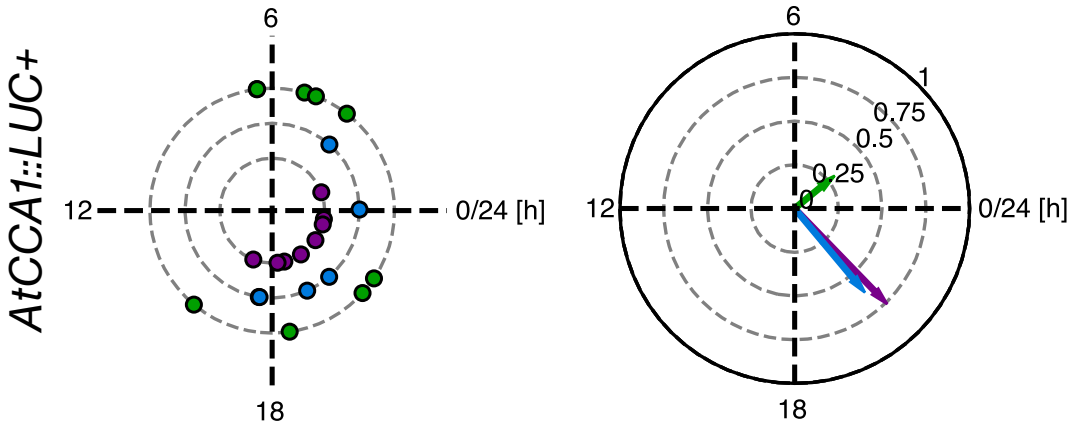

(d)

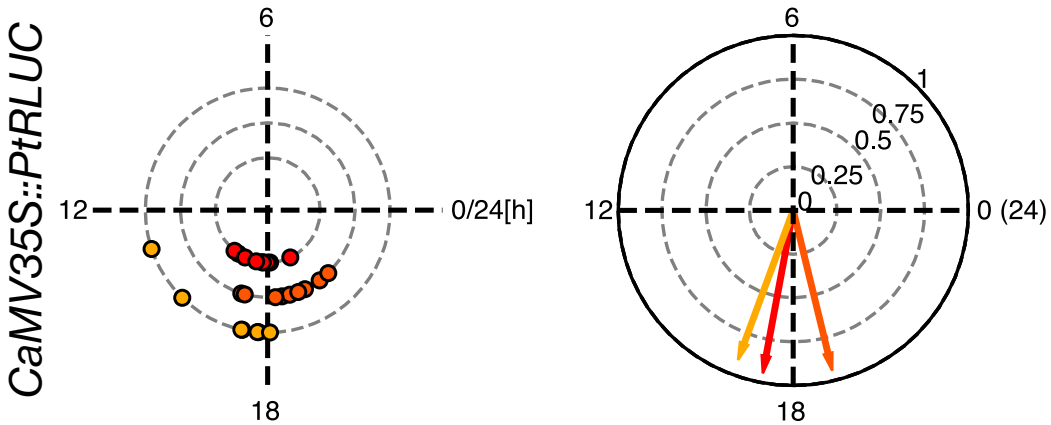

Figure S12.

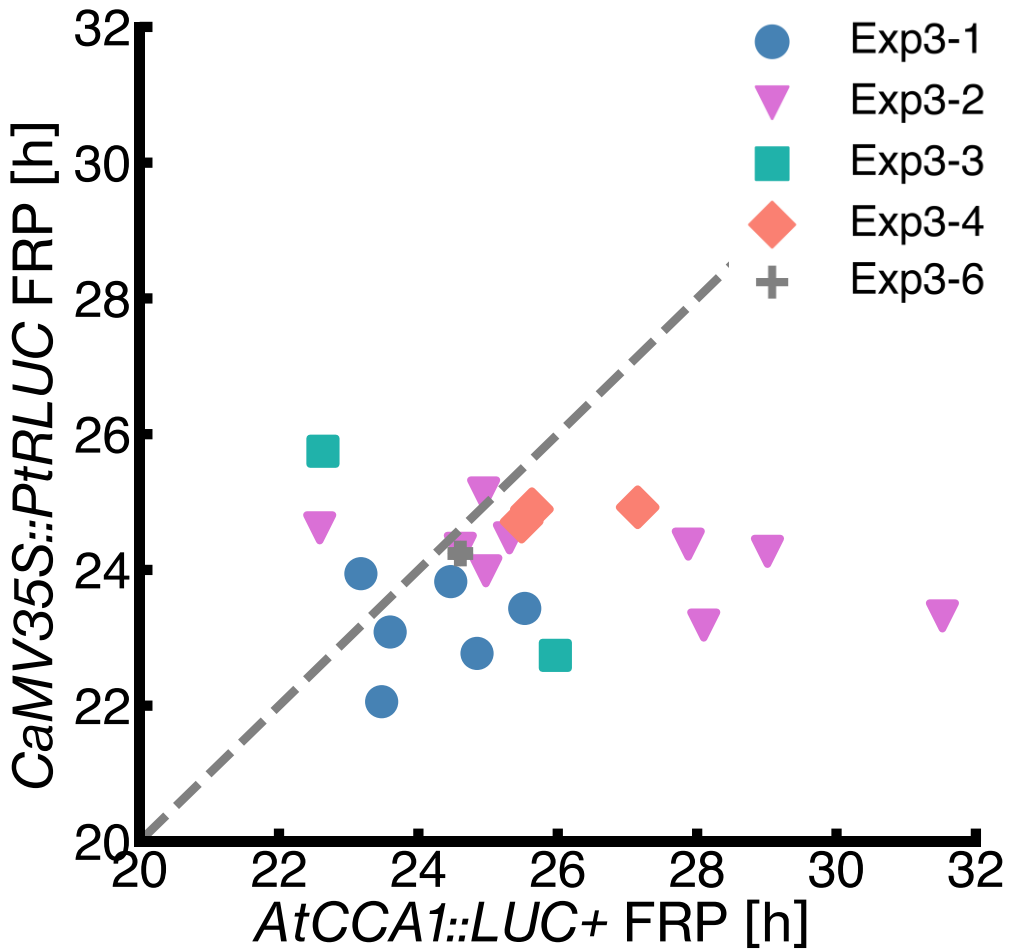
Exp3-1
Exp3-2
Exp3-3
Exp3-4
Exp3-6
CaMV35S::PtRLUC FRP [h]
AtCCA1::LUC+ FRP [h]
20
22
24
26
28
30
32

Table S1. Summary of the quantitative analysis of cellular bioluminescence rhythms.

					AtCCA1::LUC+			*CaMV35S::PtRLUC*		
Experiment name	Reporter	# Luminous cells	# Analyzable cells	# Rhythmic in both reporters	# Rhythmic cells	Proportion of rhythmic cells	FRP (h)*	# Rhythmic cells	Proportion of rhythmic cells	FRP (h)*
Exp1-1	*AtCCA1::LUC+*	28	27	-	26	0.96	25.4 ± 1.4	-	-	-
Exp1-2	*AtCCA1::LUC+*	31	30	-	28	0.93	25.1 ± 2.1	-	-	-
Exp1-3	*AtCCA1::LUC+*	36	33	-	32	0.97	26.6 ± 3.3	-	-	-
Exp1-4	*AtCCA1::LUC+*	34	33	-	32	0.97	25.4 ± 3.6	-	-	-
Exp2-1	*CaMV35S::PtRLUC*	38	38	-	-	-	-	21	0.55	24.3 ± 1.4
Exp2-2	*CaMV35S::PtRLUC*	59	59	-	-	-	-	31	0.53	24.4 ± 0.9
Exp2-3	*CaMV35S::PtRLUC*	41	41	-	-	-	-	21	0.51	26.3 ± 1.2
Exp2-4	*CaMV35S::PtRLUC*	24	24	-	-	-	-	7	0.29	24.4 ± 0.7
Exp3-1	*AtCCA1::LUC+* *CaMV35S::PtRLUC*	36	19	6	16	0.84	24.6 ± 1.0 (24.2 ± 0.8)	8	0.42	23.5 ± 1.2 (23.2 ± 0.6)
Exp3-2	*AtCCA1::LUC+* *CaMV35S::PtRLUC*	45	20	9	18	0.9	25.9 ± 2.1 (26.5 ± 2.6)	11	0.55	24.0 ± 0.7 (24.2 ± 0.6)
Exp3-3	*AtCCA1::LUC+* *CaMV35S::PtRLUC*	29	19	2	14	0.74	24.9 ± 2.1 (24.3 ± 1.7)	2	0.11	24.2 ± 1.5 (24.2 ± 1.5)
Exp3-4	*AtCCA1::LUC+* *CaMV35S::PtRLUC*	25	8	3	7	0.88	26.4 ± 1.0 (26.1 ± 0.8)	3	0.38	24.8 ± 0.1 (24.8 ± 0.1)
Exp3-5	*AtCCA1::LUC+* *CaMV35S::PtRLUC*	25	3	0	2	0.67	25.5 ± 2.6	0	0	-
Exp3-6	*AtCCA1::LUC+* *CaMV35S::PtRLUC*	29	4	1	3	0.75	24.9 ± 0.4 (24.6)	1	0.25	24.2 (24.2)

* Mean FRP ± SD for cells with circadian rhythms in both reporters is shown in the parantasis.